

OPTIMAL ACTUATOR DESIGN BASED ON SHAPE CALCULUS*

DANTE KALISE[†], KARL KUNISCH[‡], AND KEVIN STURM[§]

Abstract. An approach to optimal actuator design based on shape and topology optimisation techniques is presented. For linear diffusion equations, two scenarios are considered. For the first one, best actuators are determined depending on a given initial condition. In the second scenario, optimal actuators are determined based on all initial conditions not exceeding a chosen norm. Shape and topological sensitivities of these cost functionals are determined. A numerical algorithm for optimal actuator design based on the sensitivities and a level-set method is presented. Numerical results support the proposed methodology.

Key words. shape optimization, feedback control, topological derivative, shape derivative, level-set method

AMS subject classifications. 49Q10, 49M05, 93B40, 65D99, 93C20.

1. Introduction. In engineering, an actuator is a device transforming an external signal into a relevant form of energy for the system in which it is embedded. Actuators can be mechanical, electrical, hydraulic, or magnetic, and are fundamental in the control loop, as they materialise the control action within the physical system. Driven by the need to improve the performance of a control setting, actuator/sensor positioning and design is an important task in modern control engineering which also constitutes a challenging mathematical topic. Optimal actuator positioning and design departs from the standard control design problem where the actuator configuration is known a priori, and addresses a higher hierarchy problem, namely, the optimisation of the *control to state map*.

There is no unique framework which is followed to address optimal actuator problems. However, concepts which immediately suggest themselves -at least for linear dynamics- and which have been addressed in the literature, build on choosing actuator design in such a manner that stabilization or controllability are optimized by an appropriate choice of the controller. This can involve Riccati equations from linear-quadratic regulator theory, and appropriately chosen parameterizations of the set of admissible actuators. The present work partially relates to this stream as we optimise the actuator design based on the performance of the resulting control loop. Within this framework, we follow a distinctly different approach by casting the optimal actuator design problem as shape and topology optimisation problems. The class of admissible actuators are characteristic functions of measurable sets and their shape is determined by techniques from shape calculus and optimal control. The class of cost functionals which we consider within this work are quadratic ones and account for the stabilization of the closed-loop dynamics. We present the concepts here for the linear heat equation, but the techniques can be extended to more general classes of functionals and stabilizable dynamical systems. We believe that the concepts of

*

Funding: D.K. and K.K. were partially funded by the ERC Advanced Grant OCLOC.

[†]Department of Mathematics, Imperial College London, South Kensington Campus, London SW7 2AZ, United Kingdom (dkaliseb@ic.ac.uk),

[‡]Johann Radon Institute for Computational and Applied Mathematics, Austrian Academy of Sciences & Institute of Analysis and Scientific Computing, University of Graz, Heinrichstr. 36, 8010 Graz, Austria (karl.kunisch@uni-graz.at)

[§]Institute for Analysis and Scientific Computing, TU Wien, Wiedner Hauptstr. 8-10, 1040 Wien, Austria (kevin.sturm@tuwien.ac.at).

39 shape and topology optimisation constitute an important tool for solving actuator
 40 positioning problems, and to our knowledge this can be the first step towards this
 41 direction. More concretely, our contributions in this paper are:

- 42 i) We study an optimal actuator design problem for linear diffusion equations.
 43 In our setting, actuators are parametrised as indicator functions over a sub-
 44 domain, and are evaluated according to the resulting closed-loop performance
 45 for a given initial condition, or among a set of admissible initial conditions
 46 not exceeding a certain norm.
- 47 ii) By borrowing a leaf from shape calculus, we derive shape and topological
 48 sensitivities for the optimal actuator design problem.
- 49 iii) Based on the formulas obtained in ii), we construct a gradient-based and a
 50 level-set method for the numerical realisation of optimal actuators.
- 51 iv) We present a numerical validation of the proposed computational method-
 52 ology. Most notably, our numerical experiments indicate that throughout
 53 the proposed framework we obtain non-trivial, multi-component actuators,
 54 which would be otherwise difficult to forecast based on tuning, heuristics, or
 55 experts' knowledge.

56 Let us, very briefly comment on the related literature. Most of these endeavors
 57 focus on control problems related to ordinary differential equations. We quote the two
 58 surveys papers [12, 27] and [26]. From these publications already it becomes clear that
 59 the notion by which optimality is measured is an important topic in its own right.
 60 The literature on optimal actuator positioning for distributed parameter systems is
 61 less rich but it also dates back for several decades already. From among the earlier
 62 contributions we quote [9] where the topic is investigated in a semigroup setting for
 63 linear systems, [5] for a class of linear infinite dimensional filtering problems, and [11]
 64 where the optimal actuator problem is investigated for hyperbolic problems related to
 65 active noise suppression. In the works [18, 16, 19] the optimal actuator problem is for-
 66 mulated in terms of parameter-dependent linear quadratic regulator problems where
 67 the parameters characterize the position of actuators, with predetermined shape, for
 68 example. By choosing the actuator position in [13] the authors optimise the decay
 69 rate in the one-dimensional wave equation. Our research may be most closely related
 70 to the recent contribution [21], where the optimal actuator design is driven by exact
 71 controllability considerations, leading to actuators which are chosen on the basis of
 72 minimal energy controls steering the system to zero within a specified time uniformly,
 73 for a bounded set of initial conditions. Finally, let us mention that the optimal actu-
 74 ator problem is in some sense dual to optimal sensor location problems [14], which is
 75 of paramount importance.

76 *Structure of the paper.* The paper is organised as follows.

77 In Section 2, the optimal control problems, with respect to which optimal ac-
 78 tuators are sought later, are introduced. While the first formulation depends on a
 79 single initial condition for the system dynamics, in the second formulation the optimal
 80 actuator mitigates the worst closed-loop performance among all the possible initial
 81 conditions.

82 In Sections 3 and 4 we derive the shape and topological sensitivities associated
 83 to the aforedescribed optimal actuator design problems.

84 Section 5 is devoted to describing a numerical approach which constructs the
 85 optimal actuator based on the shape and topological derivatives computed in Sections
 86 3 and 4. It involves the numerical realisation of the sensitivities and iterative gradient-
 87 based and level-set approaches.

88 Finally in Section 6 we report on computations involving numerical tests for our

89 model problem in dimensions one and two.

90 **1.1. Notation.** Let $\Omega \subset \mathbf{R}^d$, $d = 1, 2, 3$ be either a bounded domain with $C^{1,1}$
 91 boundary $\partial\Omega$ or a convex domain, and let $T > 0$ be a fixed time. The space-time
 92 cylinder is denoted by $\Omega_T := \Omega \times (0, T]$. Further by $H^1(\Omega)$ denotes the Sobolev
 93 space of square integrable functions on Ω with square integrable weak derivative.
 94 The space $H_0^1(\Omega)$ comprises all functions in $H^1(\Omega)$ that have trace zero on $\partial\Omega$ and
 95 $H^{-1}(\Omega)$ stands for the dual of $H_0^1(\Omega)$. The space $\mathring{C}^{0,1}(\bar{\Omega}, \mathbf{R}^d)$ comprises all Lipschitz
 96 continuous functions on $\bar{\Omega}$ vanishing on $\partial\Omega$. It is a closed subspace of $C^{0,1}(\bar{\Omega}, \mathbf{R}^d)$,
 97 the space of Lipschitz continuous mappings defined on $\bar{\Omega}$. Similarly we denote by
 98 $\mathring{C}^k(\bar{\Omega}, \mathbf{R}^d)$ all k -times differentiable functions on $\bar{\Omega}$ vanishing on $\partial\Omega$. We use the
 99 notation ∂f for the Jacobian of a function f . Further $B_\epsilon(x)$ stands for the open ball
 100 centered at $x \in \mathbf{R}^d$ with radius $\epsilon > 0$. Its closure is denoted $\bar{B}_\epsilon(x) := \overline{B_\epsilon(x)}$. By
 101 $\mathfrak{Y}(\Omega)$ we denote the set of all measurable subsets $\omega \subset \Omega$. We say that a sequence (ω_n)
 102 in $\mathfrak{Y}(\Omega)$ converges to an element $\omega \in \mathfrak{Y}(\Omega)$ if $\chi_{\omega_n} \rightarrow \chi_\omega$ in $L_1(\Omega)$ as $n \rightarrow \infty$, where
 103 χ_ω denotes the characteristic function of ω . In this case we write $\omega_n \rightarrow \omega$. Notice
 104 that $\chi_{\omega_n} \rightarrow \chi_\omega$ in $L_1(\Omega)$ as $n \rightarrow \infty$ if and only if $\chi_{\omega_n} \rightarrow \chi_\omega$ in $L_p(\Omega)$ as $n \rightarrow \infty$ for
 105 all $p \in [1, \infty)$. For two sets $A, B \subset \mathbf{R}^d$ we write $A \Subset B$ if A is compact and $\bar{A} \subset B$.

106 2. Problem formulation and first properties.

107 **2.1. Problem formulation.** Our goal is to study an optimal actor positioning
 108 and design problem for a controlled linear parabolic equation. Let \mathcal{U} be a closed and
 109 convex subset of $L_2(\Omega)$ with $0 \in \mathcal{U}$. For each $\omega \in \mathfrak{Y}(\Omega)$ the set $\chi_\omega \mathcal{U}$ is a convex
 110 subset of $L_2(\Omega)$. The elements of the space $\mathfrak{Y}(\Omega)$ are referred to as *actuators*. The
 111 choices $\mathcal{U} = L_2(\Omega)$ and $\mathcal{U} = \mathbf{R}$, considered as the space of constant functions on Ω ,
 112 will play a special role. Further, $\mathbf{U} := L_2(0, T; \mathcal{U})$ denotes the space of time-dependent
 113 controls, which is equipped with the topology induced by the $L_2(0, T; L_2(\Omega))$ -norm.
 114 We denote by K a nonempty, weakly closed subset of $H_0^1(\Omega)$. It will serve as the
 115 set of admissible initial conditions for the stable formulation of our optimal actuator
 116 positioning problem.

117 With these preliminaries we consider for every triplet $(\omega, u, f) \in \mathfrak{Y}(\Omega) \times \mathbf{U} \times H_0^1(\Omega)$
 118 the following linear parabolic equation: find $y : \bar{\Omega} \times [0, T] \rightarrow \mathbf{R}$ satisfying

$$\begin{aligned} 119 \quad (1a) \quad & \partial_t y - \Delta y = \chi_\omega u && \text{in } \Omega \times (0, T], \\ 120 \quad (1b) \quad & y = 0 && \text{on } \partial\Omega \times (0, T], \\ 121 \quad (1c) \quad & y(0) = f && \text{on } \Omega. \end{aligned}$$

123 In the following, we discuss the well-posedness of the system dynamics 1 and the asso-
 124 ciated linear-quadratic optimal control problem, to finally state the optimal actuator
 125 design problem.

126 *Well-posedness of the linear parabolic problem.* It is a classical result [10, p. 356,
 127 Theorem 3] that system (1) admits a unique weak solution $y = y^{u,f,\omega}$ in $W(0, T)$,
 128 where

$$129 \quad W(0, T) := \{y \in L_2(0, T; H_0^1(\Omega)) : \partial_t y \in L_2(0, T; H^{-1}(\Omega))\},$$

130 which satisfies by definition,

$$131 \quad (2) \quad \langle \partial_t y, \varphi \rangle_{H^{-1}, H_0^1} + \int_{\Omega} \nabla y \cdot \nabla \varphi \, dx = \int_{\Omega} \chi_\omega u \varphi \, dx$$

132 for all $\varphi \in H_0^1(\Omega)$ for a.e. $t \in (0, T]$, and $y(0) = f$. For the shape calculus of Section 4
 133 we require that $f \in H_0^1(\Omega)$. In this case the state variable enjoys additional regularity

134 properties. In fact, in [10, p. 360, Theorem 5] it is shown that for $f \in H_0^1(\Omega)$ the
135 weak solution $y^{\omega,u,f}$ satisfies

$$136 \quad (3) \quad y^{u,f,\omega} \in L_2(0, T, H^2(\Omega)) \cap L_\infty(0, T; H_0^1(\Omega)), \quad \partial_t y^{u,f,\omega} \in L_2(0, T; L_2(\Omega))$$

137 and there is a constant $c > 0$, independent of ω, f and u , such that

$$138 \quad (4) \quad \|y^{u,f,\omega}\|_{L_\infty(H^1)} + \|y^{u,f,\omega}\|_{L_2(H^2)} + \|\partial_t y^{u,f,\omega}\|_{L_2(L_2)} \leq c(\|\chi_\omega u\|_{L_2(L_2)} + \|f\|_{H^1}).$$

139 Thanks to the lemma of Aubin-Lions the space

$$140 \quad (5) \quad Z(0, T) := \{y \in L_2(0, T; H^2(\Omega)) \cap H_0^1(\Omega) : \partial_t y \in L_2(0, T; L^2(\Omega))\}$$

141 is compactly embedded into $L_\infty(0, T; H_0^1(\Omega))$.

142 *The linear-quadratic optimal control problem.* After having discussed the well-
143 posedness of the linear parabolic problem, we recall a standard linear-quadratic opti-
144 mal control problem associated to a given actuator ω . Let $\gamma > 0$ be given. First we
145 define for every triplet $(\omega, f, u) \in \mathfrak{Y}(\Omega) \times H_0^1(\Omega) \times U$ the cost functional

$$146 \quad (6) \quad J(\omega, u, f) := \int_0^T \|y^{u,f,\omega}(t)\|_{L_2(\Omega)}^2 + \gamma \|u(t)\|_{L_2(\Omega)}^2 dt.$$

147 By taking the infimum in (6) over all controls $u \in U$ we obtain the function \mathcal{J}_1 , which
148 is defined for all $(\omega, f) \in \mathfrak{Y}(\Omega) \times H_0^1(\Omega)$:

$$149 \quad (7) \quad \mathcal{J}_1(\omega, f) := \inf_{u \in U} J(\omega, u, f).$$

150 It is well known, see e.g. [25] that the minimisation problem on the right hand
151 side of (7), constrained to the dynamics (1) admits a unique solution. As a result,
152 the function $\mathcal{J}_1(\omega, f)$ is well-defined. The minimiser \bar{u} of (7) depends on the initial
153 condition f and the set ω , i.e., $\bar{u} = \bar{u}^{\omega,f}$. In order to eliminate the dependence of the
154 optimal actuator ω on the initial condition f we define a robust function \mathcal{J}_2 by taking
155 the supremum in (7) over all normalized initial conditions f in K :

$$156 \quad (8) \quad \mathcal{J}_2(\omega) := \sup_{\substack{f \in K, \\ \|f\|_{H_0^1(\Omega)} \leq 1}} \mathcal{J}_1(\omega, f).$$

157 We show later on that the supremum on the right hand side of (8) is actually attained.

158 *The optimal actuator design problem.* We now have all the ingredients to state the
159 optimal actuator design problem we shall study in the present work. In the subsequent
160 sections we are concerned with the following minimisation problem

$$161 \quad (9) \quad \inf_{\substack{\omega \in \mathfrak{Y}(\Omega) \\ |\omega|=c}} \mathcal{J}_1(\omega, f), \quad \text{for } f \in K,$$

162 where $c \in (0, |\Omega|)$ is the measure of the prescribed volume of the actuator ω . That is,
163 for a given initial condition f and a given volume constraint c , we design the actuator
164 ω according to the closed-loop performance of the resulting linear-quadratic control
165 problem (7). Note that no further constraint concerning the actuator topology is
166 considered. Buidling upon this problem, we shall also study the problem

$$167 \quad (10) \quad \inf_{\substack{\omega \in \mathfrak{Y}(\Omega) \\ |\omega|=c}} \mathcal{J}_2(\omega),$$

168 where the dependence of the optimal actuator on the initial condition of the dynamics
169 is removed by minimising among the set of all the normalised initial condition $f \in K$.

170 Finally, another problem of interest which can be studied within the present
171 framework is the *optimal actuator positioning* problem, where the topology of the
172 actuator is fixed, and only its position is optimised. Given a fixed set $\omega_0 \subset \Omega$ we
173 study the optimal actuator positioning problem by solving

$$174 \quad (11) \quad \inf_{X \in \mathbf{R}^d} \mathcal{J}_1((\text{id} + X)(\omega_0), f), \text{ for } f \in K,$$

175 and

$$176 \quad (12) \quad \inf_{X \in \mathbf{R}^d} \mathcal{J}_2((\text{id} + X)(\omega_0)),$$

177 where $(\text{id} + X)(\omega_0) = \{x + X : x \in \omega_0\}$, i.e., we restrict our optimisation procedure
178 to a set of actuator translations.

179 Our goal is to characterize shape and topological derivatives for $\mathcal{J}_1(\omega, f)$ (for
180 fixed f) and $\mathcal{J}_2(\omega)$ in order to develop gradient type algorithms to solve (9) and (10).
181 The results presented in Sections 3 and 4 can also be utilized to derive optimality
182 conditions for problems (11) and (12). In addition, we investigate numerically whether
183 the proposed methodology provides results which coincide with physical intuition.

184 While the existence of optimal shapes according to (9) and (10) is certainly also
185 an interesting task, this issue is postponed to future work. We mention [21] where a
186 problem similar to ours but with different cost functional is considered.

187 **2.2. Optimality system for \mathcal{J}_1 .** The unique solution $\bar{u} \in U$ of the minimisation
188 problem on the right hand side of (7) can be characterised by the first order necessary
189 optimality condition

$$190 \quad (13) \quad \partial_u J(\omega, \bar{u}, f)(v - \bar{u}) \geq 0 \quad \text{for all } v \in U.$$

191 The function $\bar{u} \in U$ satisfies the variational inequality (13) if and only if there is a
192 multiplier $\bar{p} \in W(0, T)$ such that the triplet $(\bar{u}, \bar{y}, \bar{p}) \in U \times W(0, T) \times W(0, T)$ solves

$$193 \quad (14a) \quad \int_{\Omega_T} \partial_t \bar{y} \varphi + \nabla \bar{y} \cdot \nabla \varphi \, dx \, dt = \int_{\Omega_T} \chi_\omega \bar{u} \varphi \, dx \, dt \quad \text{for all } \varphi \in W(0, T),$$

$$194 \quad (14b) \quad \int_{\Omega_T} \partial_t \psi \bar{p} + \nabla \psi \cdot \nabla \bar{p} \, dx \, dt = - \int_{\Omega_T} 2\bar{y} \psi \, dx \, dt \quad \text{for all } \psi \in W(0, T),$$

$$195 \quad (14c) \quad \int_{\Omega} (2\gamma \bar{u} - \chi_\omega \bar{p})(v - \bar{u}) \, dx \geq 0 \quad \text{for all } v \in U, \quad \text{a.e. } t \in (0, T),$$

196
197 supplemented with the initial and terminal conditions $\bar{y}(0) = f$ and $\bar{p}(T) = 0$ a.e. in
198 Ω . Two cases are of particular interest to us:

199 **REMARK 2.1.** (a) If $U = L_2(\Omega)$, then (14c) is equivalent to $2\gamma \bar{u} = \chi_\omega \bar{p}$ a.e.
200 on $\Omega \times (0, T)$.

201 (b) If $U = \mathbf{R}$, then (14c) is equivalent to $2\gamma \bar{u} = \int_\omega \bar{p} \, dx$ a.e. on $(0, T)$.

202 **2.3. Well-posedness of \mathcal{J}_2 .** Given $\omega \in \mathfrak{Y}(\Omega)$ and $f \in K$, we use the notation
203 $\bar{u}^{f, \omega}$ to denote the unique minimiser of $J(\omega, \cdot, f)$ over U .

204 **LEMMA 2.2.** Let (f_n) be a sequence in K that converges weakly in $H_0^1(\Omega)$ to $f \in$
205 K , let (ω_n) be a sequence in $\mathfrak{Y}(\Omega)$ that converges to $\omega \in \mathfrak{Y}(\Omega)$, and let (u_n) be a
206 sequence in U that converges weakly to a function $u \in U$. Then we have

$$207 \quad (15) \quad \begin{aligned} & y^{u_n, f_n, \omega_n} \rightharpoonup y^{u, f, \omega} \quad \text{in } L_2(0, T; H_0^1(\Omega)) \quad \text{as } n \rightarrow \infty, \\ & y^{u_n, f_n, \omega_n} \rightharpoonup y^{u, f, \omega} \quad \text{in } L_2(0, T; H^2(\Omega) \cap H_0^1(\Omega)) \quad \text{as } n \rightarrow \infty. \end{aligned}$$

208 *Proof.* The a-priori estimate (4) and the compact embedding $Z(0, T) \subset$
 209 $L_2(0, T; H_0^1(\Omega))$ show that we can extract a subsequence of (y^{u_n, f_n, ω_n}) that converges
 210 weakly to an element y in $L_2(0, T; H^2(\Omega) \cap H_0^1(\Omega))$ and strongly in $L_2(0, T; H_0^1(\Omega))$.
 211 Using this to pass to the limit in (2) with (u, f, ω) replaced by (u_n, f_n, ω_n) implies by
 212 uniqueness that $y = y^{u, f, \omega}$. \square

213 **LEMMA 2.3.** *Let (f_n) be a sequence in $H_0^1(\Omega)$ converging weakly to $f \in H_0^1(\Omega)$*
 214 *and let (ω_n) be a sequence in $\mathfrak{Y}(\Omega)$ that converges to $\omega \in \mathfrak{Y}(\Omega)$. Then we have*

$$215 \quad (16) \quad \bar{u}^{f_n, \omega_n} \rightarrow \bar{u}^{f, \omega} \quad \text{in } L_2(0, T; L_2(\Omega)) \text{ as } n \rightarrow \infty.$$

216 *Proof.* Using estimate (4) we see that for all $u \in \mathcal{U}$ and $n \geq 0$, we have

$$217 \quad (17) \quad \begin{aligned} & \int_0^T \|y^{\bar{u}^{f_n, \omega_n}, f_n, \omega_n}(t)\|_{L_2(\Omega)}^2 + \gamma \|\bar{u}^{f_n, \omega_n}(t)\|_{L_2(\Omega)}^2 dt \\ & \leq \int_0^T \|y^{u, f_n, \omega_n}(t)\|_{L_2(\Omega)}^2 + \gamma \|u(t)\|_{L_2(\Omega)}^2 dt \\ & \leq c(\|\chi_{\omega_n} u\|_{L_2(L_2)}^2 + \|f_n\|_{H^1}^2). \end{aligned}$$

218 It follows that $(\bar{u}_n) := (\bar{u}^{f_n, \omega_n})$ is bounded in $L_2(0, T; L_2(\Omega))$ and hence there is an
 219 element $\bar{u} \in L_2(0, T; L_2(\Omega))$ and a subsequence (\bar{u}_{n_k}) , $\bar{u}_{n_k} \rightharpoonup \bar{u}$ in $L_2(0, T; L_2(\Omega))$
 220 as $k \rightarrow \infty$. In addition this subsequence satisfies $\liminf_{k \rightarrow \infty} \|\bar{u}_{n_k}\|_{L_2(0, T; L_2(\Omega))} \geq$
 221 $\|\bar{u}\|_{L_2(0, T; L_2(\Omega))}$. Since \mathcal{U} is closed we also have $\bar{u} \in L_2(0, T; \mathcal{U})$. Together with
 222 Lemma 2.2 we therefore obtain from (17) by taking the lim inf on both sides,

$$223 \quad (18) \quad \int_0^T \|y^{\bar{u}, f, \omega}(t)\|_{L_2(\Omega)}^2 + \gamma \|\bar{u}(t)\|_{L_2(\Omega)}^2 dt \leq \int_0^T \|y^{u, f, \omega}(t)\|_{L_2(\Omega)}^2 + \gamma \|u(t)\|_{L_2(\Omega)}^2 dt$$

224 for all $u \in \mathcal{U}$. This shows that $\bar{u} = \bar{u}^{f, \omega}$ and since $\bar{u}^{f, \omega}$ is the unique minimiser
 225 of $J(\omega, \cdot, y)$ the whole sequence (\bar{u}_n) converges weakly to $\bar{u}^{f, \omega}$. In addition it follows
 226 from the strong convergence $y^{\bar{u}^{f_n, \omega_n}, f_n, \omega_n} \rightarrow y^{\bar{u}^{f, \omega}, f, \omega}$ in $W(0, T)$ and estimate (17) that
 227 the norm $\|\bar{u}^{f_n, \omega_n}\|_{L_2(0, T; L_2(\Omega))}$ converges to $\|\bar{u}^{f, \omega}\|_{L_2(0, T; L_2(\Omega))}$. As norm convergence
 228 together with weak convergence imply strong convergence, this shows that \bar{u}^{f_n, ω_n}
 229 converges strongly to $\bar{u}^{f, \omega}$ in $L_2(0, T; L_2(\Omega))$ as was to be shown. \square

230 We now prove that $\omega \mapsto \mathcal{J}_2(\omega)$ is well-defined on $\mathfrak{Y}(\Omega)$.

231 **LEMMA 2.4.** *For every $\omega \in \mathfrak{Y}(\Omega)$ there exists $f \in K$ satisfying $\|f\|_{H_0^1(\Omega)} \leq 1$ and*

$$232 \quad (19) \quad \mathcal{J}_2(\omega) = \mathcal{J}_1(\omega, f).$$

233 *Proof.* Let $\omega \in \mathfrak{Y}(\Omega)$ be fixed. In view of $0 \in \mathcal{U}$ and (4) and since $K \subset H_0^1(\Omega) \hookrightarrow$
 234 $H_0^1(\Omega)$ we obtain for all $f \in H_0^1(\Omega)$ with $\|f\|_{H_0^1(\Omega)} \leq 1$,

$$235 \quad (20) \quad \mathcal{J}_1(\omega, f) = \min_{u \in \mathcal{U}} J(\omega, u, f) \leq \int_0^T \|y^{0, f, \omega}(t)\|_{L_2(\Omega)}^2 dt \leq c\|f\|_{H_0^1(\Omega)}^2 \leq cr^2.$$

236 Further we can express \mathcal{J}_2 as follows

$$237 \quad (21) \quad \mathcal{J}_2(\omega) = \sup_{\substack{f \in K \\ \|f\|_{H_0^1(\Omega)} \leq 1}} \int_0^T \|y^{\bar{u}^{f, \omega}, f, \omega}(t)\|_{L_2(\Omega)}^2 + \gamma \|\bar{u}^{f, \omega}(t)\|_{L_2(\Omega)}^2 dt.$$

238 Let $(f_n) \subset K$, $\|f_n\|_{H_0^1(\Omega)} \leq 1$ be a maximising sequence, that is,

$$239 \quad (22) \quad \mathcal{J}_2(\omega) = \lim_{n \rightarrow \infty} \int_0^T \|y^{\bar{u}^{\omega, f_n, f_n, \omega}}(t)\|_{L_2(\Omega)}^2 + \gamma \|\bar{u}^{\omega, f_n}(t)\|_{L_2(\Omega)}^2 dt.$$

240 The sequence (f_n) is bounded in K and therefore we find a subsequence (f_{n_k}) converg-
 241 ing weakly to an element $f \in K$. Additionally, the limit element satisfies $\|f\|_{H_0^1(\Omega)} \leq$
 242 $\liminf_{k \rightarrow \infty} \|f_{n_k}\|_{H_0^1(\Omega)} \leq 1$ and hence $\|f\|_{H_0^1(\Omega)} \leq 1$. Since (f_{n_k}) is also bounded in
 243 $H_0^1(\Omega)$ we may assume that (f_{n_k}) also converges weakly to $f \in H_0^1(\Omega)$. Thanks to
 244 Lemmas 2.3 and 2.2 we obtain

$$245 \quad (23) \quad \begin{aligned} \mathcal{J}_2(\omega) &= \lim_{k \rightarrow \infty} \int_0^T \|y^{\bar{u}^{f_{n_k}, \omega, f_{n_k}, \omega}}(t)\|_{L_2(\Omega)}^2 + \gamma \|\bar{u}^{f_{n_k}, \omega}(t)\|_{L_2(\Omega)}^2 dt \\ &= \int_0^T \|y^{\bar{u}^{f, \omega, f, \omega}}(t)\|_{L_2(\Omega)}^2 + \gamma \|\bar{u}^{f, \omega}(t)\|_{L_2(\Omega)}^2 dt. \end{aligned} \quad \square$$

246 **REMARK 2.5.** In view of Lemma 2.4 we write from now on $\mathcal{J}_2(\omega) =$
 247 $\max_{\substack{f \in K, \\ \|f\|_{H_0^1(\Omega)} \leq 1}} \mathcal{J}_1(\omega, f)$.

248 **3. Shape derivative.** In this section we prove the directional differentiability
 249 of \mathcal{J}_2 at arbitrary measurable sets. We employ the averaged adjoint approach [23]
 250 which is tailored to the derivation of directional derivatives of PDE constrained shape
 251 functions. Moreover this approach allows us later on to also compute the topological
 252 derivative of \mathcal{J}_1 and \mathcal{J}_2 without performing asymptotic analysis which can otherwise
 253 be quite involved [20].

254 Of course, there are notable alternative approaches, most prominent the material
 255 derivative approach, to prove directional differentiability of shape functions, see e.g.
 256 [15, 6]. For an overview of available methods the reader may consult [24].

257 **3.1. Shape derivative.** Given a vector field $X \in \mathring{C}^{0,1}(\bar{\Omega}, \mathbf{R}^d)$, we denote by
 258 T_t^X the perturbation of the identity $T_t^X(x) := x + tX(x)$ which is bi-Lipschitz for all
 259 $t \in [0, \tau_X]$, where $\tau_X := 1/(2\|X\|_{C^{0,1}})$. We omit the index X and write T_t instead
 260 of T_t^X whenever no confusion is possible. A mapping $J : \mathfrak{J}(\Omega) \rightarrow \mathbf{R}$ is called *shape*
 261 *function*.

262 **DEFINITION 3.1.** The directional derivative of J at $\omega \in \mathfrak{J}(\Omega)$ in direction $X \in$
 263 $\mathring{C}^{0,1}(\bar{\Omega}, \mathbf{R}^d)$ is defined by

$$264 \quad (24) \quad DJ(\omega)(X) := \lim_{t \searrow 0} \frac{J(T_t(\omega)) - J(\omega)}{t}.$$

265 We say that J is

- 266 (i) directionally differentiable at ω (in $\mathring{C}^{0,1}(\bar{\Omega}, \mathbf{R}^d)$), if $DJ(\omega)(X)$ exists for all
- 267 $X \in \mathring{C}^{0,1}(\bar{\Omega}, \mathbf{R}^d)$,
- 268 (ii) differentiable at ω (in $\mathring{C}^{0,1}(\bar{\Omega}, \mathbf{R}^d)$), if $DJ(\omega)(X)$ exists for all
- 269 $X \in \mathring{C}^{0,1}(\bar{\Omega}, \mathbf{R}^d)$ and $X \mapsto DJ(\omega)(X)$ is linear and continuous.

270 The following properties will frequently be used.

271 **LEMMA 3.2.** Let $\Omega \subseteq \mathbf{R}^d$ be open and bounded and pick a vector field $X \in$
 272 $\mathring{C}^{0,1}(\bar{\Omega}, \mathbf{R}^d)$. (Note that $T_t(\Omega) = \Omega$ for all t .)

273 (i) We have as $t \rightarrow 0^+$,

$$274 \quad \frac{\partial T_t - I}{t} \rightarrow \partial X \quad \text{and} \quad \frac{\partial T_t^{-1} - I}{t} \rightarrow -\partial X \quad \text{strongly in } L_\infty(\bar{\Omega}, \mathbf{R}^{d \times d})$$

$$275 \quad \frac{\det(\partial T_t) - 1}{t} \rightarrow \operatorname{div}(X) \quad \text{strongly in } L_\infty(\bar{\Omega}).$$

277 (ii) For all $\varphi \in L_2(\Omega)$, we have as $t \rightarrow 0^+$,

$$278 \quad (25) \quad \varphi \circ T_t \rightarrow \varphi \quad \text{strongly in } L_2(\Omega).$$

280 (iii) Let (φ_n) be a sequence in $H^1(\Omega)$ that converges weakly to $\varphi \in H^1(\Omega)$. Let
281 (t_n) a null-sequence. Then we have as $n \rightarrow \infty$,

$$282 \quad (26) \quad \frac{\varphi_n \circ T_{t_n} - \varphi_n}{t_n} \rightharpoonup \nabla \varphi \cdot X \quad \text{weakly in } L_2(\Omega).$$

284 *Proof.* Item (i) is obvious. The convergence result (25) is proved in [7, Lem. 2.1,
285 p.527] and (26) can be proved in a similar fashion.

286 Item (iii) is less obvious and we give a proof. For every $\epsilon > 0$ and $\psi \in H^1(\Omega)$,
287 there is $N > 0$, such that $|(\varphi_n - \varphi, \psi)_{H^1}| \leq \epsilon$ for all $n \geq N_\epsilon$. By density we find for
288 every n and every null-sequence (ϵ_n) , $\epsilon_n > 0$ an element $\tilde{\varphi}_n \in C^1(\bar{\Omega})$, such that

$$289 \quad (27) \quad \|\tilde{\varphi}_n - \varphi_n\|_{H^1} \leq \epsilon_n.$$

290 It is clear that $\tilde{\varphi}_n \rightharpoonup \varphi$ weakly in $H^1(\Omega)$ as $n \rightarrow \infty$. We now write

$$291 \quad (28) \quad \frac{\varphi_n \circ T_{t_n} - \varphi_n}{t_n} - \nabla \varphi_n \cdot X = \frac{(\varphi_n - \tilde{\varphi}_n) \circ T_{t_n} - (\varphi_n - \tilde{\varphi}_n)}{t_n} - \nabla(\varphi_n - \tilde{\varphi}_n) \cdot X$$

$$+ \frac{\tilde{\varphi}_n \circ T_{t_n} - \tilde{\varphi}_n}{t_n} - \nabla \tilde{\varphi}_n \cdot X.$$

292 Let $x \in \Omega$. Applying the fundamental theorem of calculus to $s \mapsto \tilde{\varphi}_n(T_s(x))$ on $[0, 1]$
293 gives

$$294 \quad (29) \quad \frac{\tilde{\varphi}_n(T_{t_n}(x)) - \tilde{\varphi}_n(x)}{t_n} = \int_0^1 \nabla \tilde{\varphi}_n(x + t_n s X(x)) \cdot X(x) ds.$$

295 We now show that the function $q_n(x) := \int_0^1 \nabla \tilde{\varphi}_n(x + t_n s X(x)) \cdot X(x)$ converges weakly
296 to $\nabla \varphi \cdot X$ in $L_2(\Omega)$. For this purpose we consider for $\psi \in L_2(\Omega)$,

$$297 \quad (30) \quad \int_\Omega q_n \psi dx = \int_\Omega \int_0^1 \nabla \tilde{\varphi}_n(x + t_n s X(x)) \cdot X(x) \psi(x) ds dx.$$

298 Interchanging the order of integration and invoking a change of variables (recall
299 $T_t(\Omega) = \Omega$), we get

$$300 \quad (31) \quad \int_\Omega q_n \psi dx = \int_0^1 \int_\Omega \underbrace{\det(\partial T_{st_n}^{-1}) \nabla \tilde{\varphi}_n \cdot ((X\psi) \circ T_{st_n}^{-1})}_{:=\eta(t_n, s)} dx ds.$$

301 Owing to item (ii) and noting that $X \circ T_t^{-1} \rightarrow X$ in $L_\infty(\Omega)$ as $t \rightarrow 0$, we also have
302 for $s \in [0, 1]$ fixed,

$$303 \quad (32) \quad \det(\partial T_{st_n}^{-1})(X\psi) \circ T_{st_n}^{-1} \rightarrow X\psi \quad \text{in } L_2(\Omega, \mathbf{R}^2) \quad \text{as } n \rightarrow \infty.$$

304 As a result using the weak convergence of $(\tilde{\varphi}_n)$ in $H^1(\Omega)$, we get for $s \in [0, 1]$,

$$305 \quad (33) \quad \eta(t_n, s) \rightarrow \int_{\Omega} \nabla \varphi \cdot X \psi \, dx \quad \text{as } n \rightarrow \infty.$$

306 It is also readily checked using Hölder's inequality that $|\eta(t_n, s)| \leq c \|\nabla \tilde{\varphi}_n\|_{L_2} \|\psi\|_{L_2}$
 307 for a constant $c > 0$ independent of $s \in [0, 1]$. As a result we may apply Lebegue's
 308 dominated convergence theorem to obtain

$$309 \quad (34) \quad \int_{\Omega} q_n \psi \, dx = \int_0^1 \eta(t_n, s) \, ds \rightarrow \int_0^1 \eta(0, s) \, ds = \int_{\Omega} \nabla \varphi \cdot X \, dx \quad \text{as } n \rightarrow \infty.$$

310 This proves that q_n converges weakly to $\nabla \varphi \cdot X$.

311 Finally testing (28) with ψ , integrating over Ω and estimating gives

$$312 \quad (35) \quad \left| \left(\frac{\varphi_n \circ T_{t_n} - \varphi_n}{t_n} - \nabla \varphi_n \cdot X, \psi \right)_{L_2} \right| \\ \leq c \|\psi\|_{L_2} (\epsilon_n/t_n + \epsilon_n) + \left| \left(\frac{\tilde{\varphi}_n \circ T_{t_n} - \tilde{\varphi}_n}{t_n} - \nabla \tilde{\varphi}_n \cdot X, \psi \right)_{L_2} \right|$$

313 with a constant $c > 0$ only depending on X . Now we choose $\tilde{N}_\epsilon \geq 1$ so large that

$$314 \quad (36) \quad \left| \left(\frac{\tilde{\varphi}_n \circ T_{t_n} - \tilde{\varphi}_n}{t_n} - \nabla \varphi \cdot X, \psi \right)_{L_2} \right| \leq \epsilon \quad \text{for all } n \geq \tilde{N}_\epsilon.$$

315 Then

$$316 \quad (37) \quad \left| \left(\frac{\tilde{\varphi}_n \circ T_{t_n} - \tilde{\varphi}_n}{t_n} - \nabla \tilde{\varphi}_n \cdot X, \psi \right)_{L_2} \right| \\ \leq \epsilon + |(\nabla(\tilde{\varphi}_n - \varphi_n) \cdot X, \psi)_{L_2}| + |(\nabla(\varphi_n - \varphi) \cdot X, \psi)_{L_2}| \\ \leq \epsilon + \epsilon_n + \epsilon \quad \text{for all } n \geq \max\{N_\epsilon, \tilde{N}_\epsilon\}.$$

317 Choosing $\epsilon_n := \min\{t_n^2, \epsilon\}$ and combining the previous estimate with (35) shows the
 318 right hand side of (37) can be bounded by 3ϵ . Since $\epsilon > 0$ was arbitrary we see that
 319 (26) holds. \square

320 **3.2. First main result: the directional derivative of \mathcal{J}_2 .** Given $\omega \in \mathfrak{Y}(\Omega)$
 321 and $r > 0$, we define the set of maximisers of $\mathcal{J}_1(\omega, \cdot)$ by

$$322 \quad (38) \quad \mathfrak{X}_2(\omega) := \{\bar{f} \in K : \sup_{\substack{f \in K, \\ \|f\|_{H_0^1(\Omega)} \leq 1}} \mathcal{J}_1(\omega, f) = \mathcal{J}_1(\omega, \bar{f})\}.$$

323 The set $\mathfrak{X}_2(\omega)$ is nonempty as shown in Lemma 2.4. Before stating our first main
 324 result we make the following assumption.

325 **ASSUMPTION 3.3.** For every $X \in \mathring{C}^{0,1}(\bar{\Omega}, \mathbf{R}^d)$ and $t \in [0, \tau_X]$ we have

$$326 \quad (39) \quad u \in \mathcal{U} \iff u \circ T_t \in \mathcal{U}.$$

327 **REMARK 3.4.** Assumption 3.3 is satisfied for \mathcal{U} equal to $L_2(\Omega)$ or \mathbf{R} .

328 Under the Assumption 3.3 we have the following theorem, where we set $\bar{y}^{f,\omega} :=$
 329 $y^{\bar{u}^{\omega,f},f,\omega}$ and $\bar{p}^{f,\omega} := p^{\bar{u}^{\omega,f},f,\omega}$ for $\omega \in \mathfrak{W}(\Omega)$ and $f \in K$. Furthermore we define for
 330 $A \in \mathbf{R}^{d \times d}, B \in \mathbf{R}^{d \times d}, a, b, c \in \mathbf{R}^d$

$$331 \quad A : B = \sum_{i,j=1}^d a_{ij} b_{ij}, \quad (a \otimes b)c := (b \cdot c)a,$$

332 where a_{ij}, b_{ij} are the entries of the matrices A, B , respectively.

333 THEOREM 3.5. (a) The directional derivative of $\mathcal{J}_2(\cdot)$ at ω in direction $X \in$
 334 $\mathring{C}^{0,1}(\bar{\Omega}, \mathbf{R}^d)$ is given by

$$335 \quad (40) \quad D\mathcal{J}_2(\omega)(X) = \max_{f \in \mathfrak{X}_2(\omega)} \int_{\Omega_T} \mathbf{S}_1(\bar{y}^{f,\omega}, \bar{p}^{f,\omega}, \bar{u}^{f,\omega}) : \partial X + \mathbf{S}_0(f) \cdot X \, dx \, dt,$$

336 where the functions $\mathbf{S}_1(f) := \mathbf{S}_1(\bar{y}^{f,\omega}, \bar{p}^{f,\omega}, \bar{u}^{f,\omega})$ and $\mathbf{S}_0(f)$ are given by

$$337 \quad (41) \quad \begin{aligned} \mathbf{S}_1(f) &= I(|\bar{y}^{f,\omega}|^2 + \gamma|\bar{u}^{f,\omega}|^2 - \bar{y}^{f,\omega} \partial_t \bar{p}^{f,\omega} + \nabla \bar{y}^{f,\omega} \cdot \nabla \bar{p}^{f,\omega} - \chi_\omega \bar{u}^{f,\omega} \bar{p}^{f,\omega}) \\ &\quad - \nabla \bar{y}^{f,\omega} \otimes \nabla \bar{p}^{f,\omega} - \nabla \bar{p}^{f,\omega} \otimes \nabla \bar{y}^{f,\omega}, \\ \mathbf{S}_0(f) &= -\frac{1}{T} \nabla f \bar{p}^{f,\omega} \end{aligned}$$

338 and the adjoint $\bar{p}^{f,\omega}$ satisfies

$$339 \quad (42) \quad \partial_t \bar{p}^{f,\omega} - \Delta \bar{p}^{f,\omega} = -2\bar{y}^{f,\omega} \quad \text{in } \Omega \times (0, T],$$

$$340 \quad (43) \quad \bar{p}^{f,\omega} = 0 \quad \text{on } \partial\Omega \times (0, T],$$

$$341 \quad (44) \quad \bar{p}^{f,\omega}(T) = 0 \quad \text{in } \Omega.$$

343 (b) The directional derivative of $\mathcal{J}_1(\cdot, f)$ at ω in direction $X \in \mathring{C}^{0,1}(\bar{\Omega}, \mathbf{R}^d)$ is
 344 given by

$$345 \quad (45) \quad D\mathcal{J}_1(\omega, f)(X) = \int_{\Omega_T} \mathbf{S}_1(f) : \partial X + \mathbf{S}_0(f) \cdot X \, dx \, dt,$$

346 where $\mathbf{S}_0(f)$ and $\mathbf{S}_1(f)$ are defined by (41).

347 Proof of item (b). We notice that for $r > 0$ we have

$$348 \quad (46) \quad \max_{\substack{f \in K, \\ \|f\|_{H_0^1(\Omega)} \leq r}} \mathcal{J}_1(\omega, f) = r^2 \max_{\substack{f \in \frac{1}{r}K, \\ \|f\|_{H_0^1(\Omega)} \leq 1}} \mathcal{J}_1(\omega, f).$$

349 Therefore we may assume that $\bar{f} \in K$ with $\|\bar{f}\|_{H_0^1(\Omega)} \leq 1$. Setting $K := \{\bar{f}\}$, we have
 350 for all $\omega \in \mathfrak{W}(\Omega)$,

$$351 \quad (47) \quad \mathcal{J}_2(\omega) = \max_{\substack{f \in K, \\ \|f\|_{H_0^1(\Omega)} \leq 1}} \mathcal{J}_1(\omega, f) = \mathcal{J}_1(\omega, \bar{f})$$

352 and hence the result follows from item (a) since $\mathfrak{X}_2(\omega) = \{\bar{f}\}$ is a singleton. The proof
 353 of part (a) will be given in the following subsections. \square

354 We pause here to comment on the regularity requirements imposed on f . As can be
 355 seen from the volume expression (40) we can extend $D\mathcal{J}_1(\omega, f)$ to initial conditions f
 356 in $L_2(\Omega)$. In fact, the only term that requires weakly differentiable initial conditions
 357 is the one involving \mathbf{S}_0 and it can be rewritten as follows for a.e. $t \in [0, T]$,

$$(48) \quad \begin{aligned} \int_{\Omega} \mathbf{S}_0(t) \cdot X \, dx &= -\frac{1}{T} \int_{\Omega} \nabla f \cdot X \bar{p}^{f,\omega}(t) \, dx \\ &= \frac{1}{T} \int_{\Omega} \operatorname{div}(X) f \bar{p}^{f,\omega}(t) + f \nabla \bar{p}^{f,\omega}(t) \cdot X \, dx, \end{aligned}$$

359 where we used that $\bar{p}^{f,\omega}(t) = 0$ on $\partial\Omega$. This shows that the shape derivative $D\mathcal{J}_1(\omega, f)$
 360 can be extended to initial conditions $f \in L_2(\Omega)$. However, it is not possible to obtain
 361 the shape derivative for $f \in L_2(\Omega)$ in general. This will become clear in the proof of
 362 Theorem 3.5.

363 The next corollary shows that under certain smoothness assumptions on ω we
 364 can write the integrals (40) and (45) as integrals over $\partial\omega$.

365 **COROLLARY 3.6.** *Let $f \in K$ and $X \in \mathring{C}^{0,1}(\bar{\Omega}, \mathbf{R}^d)$ be given. Assume that $\omega \Subset \Omega$
 366 and Ω are C^2 domains. Moreover, suppose that either $\mathcal{U} = L_2(\Omega)$ or $\mathcal{U} = \mathbf{R}$.*

367 (a) *Given $f \in \mathfrak{X}_2(\omega)$ define $\hat{\mathbf{S}}_1(f) := \int_0^T \mathbf{S}_1(f)(s) \, ds$ and
 368 $\hat{\mathbf{S}}_0(f) := \int_0^T \mathbf{S}_0(f)(s) \, ds$. Then we have*

$$(49) \quad \hat{\mathbf{S}}_1(f)|_{\omega} \in W_1^1(\omega, \mathbf{R}^{d \times d}), \quad \hat{\mathbf{S}}_1(f)|_{\Omega \setminus \bar{\omega}} \in W_1^1(\Omega \setminus \bar{\omega}, \mathbf{R}^{d \times d}), \quad \hat{\mathbf{S}}_0(f)|_{\omega} \in L_2(\omega, \mathbf{R}^d),$$

370 and

$$(50) \quad -\operatorname{div}(\hat{\mathbf{S}}_1(f)) + \hat{\mathbf{S}}_0(f) = 0 \quad \text{a.e. in } \omega \cup (\Omega \setminus \bar{\omega}).$$

372 Moreover (40) can be written as

$$(51) \quad \begin{aligned} D\mathcal{J}_2(\omega)(X) &= \max_{f \in \mathfrak{X}_2(\omega)} \int_{\partial\omega} [\hat{\mathbf{S}}_1(f)\nu] \cdot X \, ds \\ &= \max_{f \in \mathfrak{X}_2(\omega)} - \int_{\partial\omega} \int_0^T \bar{u}^{\omega,f} \bar{p}^{\omega,f}(X \cdot \nu) \, dt \, ds \end{aligned}$$

374 for $X \in \mathring{C}^1(\bar{\Omega}, \mathbf{R}^d)$, with ν the outer normal to ω . Here $[\hat{\mathbf{S}}_1(f)\nu] :=$
 375 $\hat{\mathbf{S}}_1(f)|_{\omega}\nu - \hat{\mathbf{S}}_1(f)|_{\Omega \setminus \bar{\omega}}\nu$ denotes the jump of $\hat{\mathbf{S}}_1(f)\nu$ across $\partial\omega$.

376 (b) We have that (45) can be written as

$$(52) \quad D\mathcal{J}_1(\omega, f)(X) = - \int_{\partial\omega} \int_0^T \bar{u}^{\omega,f} \bar{p}^{\omega,f}(X \cdot \nu) \, dt \, ds$$

378 for $X \in \mathring{C}^1(\bar{\Omega}, \mathbf{R}^d)$.

379 Before we prove this corollary we need the following auxiliary result.

380 **LEMMA 3.7.** *Suppose that Ω is of class C^2 . For all $f \in H_0^1(\Omega)$ and $\omega \in \mathfrak{D}(\Omega)$,
 381 we have*

$$(53) \quad \int_0^T \bar{y}^{f,\omega}(t) \partial_t \bar{p}^{f,\omega}(t) \, dt \in W_1^1(\Omega), \quad \text{and} \quad \int_0^T \nabla \bar{p}^{f,\omega}(t) \cdot \nabla \bar{y}^{f,\omega}(t) \, dt \in W_1^1(\Omega).$$

383 *Proof.* From the general regularity results [28, Satz 27.5, pp. 403 and Satz
384 27.3] we have that $\bar{p}^{f,\omega} \in L_2(0, T; H^3(\Omega))$ and $\partial_t \bar{p}^{f,\omega} \in L_2(0, T; H^1(\Omega))$, and $\bar{y}^{f,\omega} \in$
385 $L_2(0, T; H^2(\Omega))$ and $\partial_t \bar{y}^{f,\omega} \in L_2(0, T; L_2(\Omega))$.

386 Observe that for almost all $t \in [0, T]$ we have $\partial_t \bar{p}^{f,\omega}(t) \in H^1(\Omega)$ and $\bar{y}^{f,\omega}(t) \in$
387 $H^2(\Omega)$. So since $H^1(\Omega) \subset L_6(\Omega)$ and $H^2(\Omega) \subset C(\bar{\Omega})$, where we use that $\Omega \subset \mathbf{R}^d$,
388 $d \leq 3$ we also have $\bar{y}^{f,\omega}(t) \partial_t \bar{p}^{f,\omega}(t) \in L_6(\Omega)$ and a.e. $t \in (0, T)$

$$389 \quad (54) \quad \|\bar{y}^{f,\omega}(t) \partial_t \bar{p}^{f,\omega}(t)\|_{L_1(\Omega)} \leq C \|\bar{y}^{f,\omega}(t)\|_{H^2(\Omega)} \|\partial_t \bar{p}^{f,\omega}(t)\|_{H^1(\Omega)}$$

390 for an constant $C > 0$. Moreover by the product rule we have

$$391 \quad (55) \quad \partial_{x_j} (\bar{y}^{f,\omega}(t) \partial_t \bar{p}^{f,\omega}(t)) = \underbrace{\partial_{x_j} (\bar{y}^{f,\omega}(t))}_{\in H^1(\Omega)} \underbrace{\partial_t \bar{p}^{f,\omega}(t)}_{\in H^1(\Omega)} + \underbrace{\bar{y}^{f,\omega}(t)}_{\in H^1(\Omega)} \underbrace{(\partial_{x_j} \partial_t \bar{p}^{f,\omega}(t))}_{\in L_2(\Omega)},$$

392 so that $\partial_{x_j} (\bar{y}^{f,\omega}(t) \partial_t \bar{p}^{f,\omega}(t)) \in L_1(\Omega)$ and

$$393 \quad (56) \quad \|\partial_{x_j} (\bar{y}^{f,\omega}(t) \partial_t \bar{p}^{f,\omega}(t))\|_{L_1(\Omega)} \leq C \|\bar{y}^{f,\omega}(t)\|_{H^1(\Omega)} \|\partial_t \bar{p}^{f,\omega}(t)\|_{H^1(\Omega)}$$

394 for some constant $C > 0$. So (54) and (56) imply that $t \mapsto \|\bar{y}^{f,\omega}(t) \partial_t \bar{p}^{f,\omega}(t)\|_{W_1^1(\Omega)}$
395 belongs to $L_1(0, T)$. This shows the left inclusion in (53). As for the right hand side
396 inclusion in (53) notice that for almost all $t \in [0, T]$ we have $\bar{p}^{f,\omega}(t) \in H^3(\Omega)$. There-
397 fore $\nabla \bar{p}^{f,\omega}(t) \in H^2(\Omega)$ and $\nabla \bar{y}^{f,\omega}(t) \in H^1(\Omega)$ and thus $\nabla \bar{y}^{f,\omega}(t) \cdot \nabla \bar{p}^{f,\omega}(t) \in L_6(\Omega)$.
398 Similarly we check that $\partial_{x_j} (\nabla \bar{y}^{f,\omega}(t) \cdot \nabla \bar{p}^{f,\omega}(t)) \in L_1(\Omega)$ and thus $t \mapsto \|\nabla \bar{y}^{f,\omega}(t) \cdot$
399 $\nabla \bar{p}^{f,\omega}(t)\|_{W_1^1(\Omega)} \in L_1(0, T)$, which gives the right hand side inclusion in (53). \square

400 *Proof of Corollary 3.6.* We assume that Theorem 3.5 holds. As a consequence of
401 Lemma 3.7 we obtain (49). Then for all $X \in C_c^1(\Omega, \mathbf{R}^d)$ satisfying $X|_{\partial\omega} = 0$ we have
402 $T_t(\omega) = (\text{id} + tX)(\omega) = \omega$ for all $t \in [0, \tau_X]$. Hence $D\mathcal{J}_2(\omega)(X) = 0$ for such vector
403 fields which gives

$$404 \quad (57) \quad 0 = D\mathcal{J}_2(\omega)(X) \geq \int_{\Omega} \hat{\mathbf{S}}_1(f) : \partial X + \hat{\mathbf{S}}_0(f) \cdot X \, dx$$

405 for all $X \in C_c^1(\Omega, \mathbf{R}^d)$ satisfying $X|_{\partial\omega} = 0$ and for all $f \in \mathfrak{X}_2(\omega)$. Since for fixed f
406 the expression in (57) is linear in X this proves

$$407 \quad (58) \quad \int_{\Omega} \hat{\mathbf{S}}_1(f) : \partial X + \hat{\mathbf{S}}_0(f) \cdot X \, dx = 0$$

408 for all $X \in C_c^1(\Omega, \mathbf{R}^d)$ satisfying $X|_{\partial\omega} = 0$ and for all $f \in \mathfrak{X}_2(\omega)$. Hence testing of
409 (58) with vector fields $X \in C_c^1(\omega, \mathbf{R}^d)$ and $X \in C_c^1(\Omega \setminus \bar{\omega}, \mathbf{R}^d)$, partial integration and
410 (49) yield the continuity equation (50). As a result, by partial integration (see e.g.
411 [17]), we get for all $X \in C_c^1(\Omega, \mathbf{R}^d)$,

$$412 \quad (59) \quad \begin{aligned} D\mathcal{J}_2(\omega)(X) &= \max_{f \in \mathfrak{X}_2(\omega)} \int_{\Omega} \hat{\mathbf{S}}_1(f) : \partial X + \hat{\mathbf{S}}_0(f) \cdot X \, dx \\ &= \max_{f \in \mathfrak{X}_2(\omega)} \left(\int_{\partial\omega} [\hat{\mathbf{S}}_1(f)\nu] \cdot X \, ds + \int_{\omega} \underbrace{(-\text{div}(\hat{\mathbf{S}}_1(f) + \hat{\mathbf{S}}_0(f)))}_{=0} \cdot X \, dx \right. \\ &\quad \left. + \int_{\Omega \setminus \bar{\omega}} \underbrace{(-\text{div}(\hat{\mathbf{S}}_1(f) + \hat{\mathbf{S}}_0(f)))}_{=0} \cdot X \, dx \right), \end{aligned}$$

413 which proves the first equality in (51). Now using Lemma 3.7 we see that $\mathbf{T}(f) :=$
 414 $\hat{\mathbf{S}}_1(f) + \int_0^T \chi_\omega \bar{u}^{f,\omega}(t) \bar{p}^{f,\omega}(t) dt$ belongs to $W_1^1(\Omega, \mathbf{R}^{d \times d})$ and hence $[\mathbf{T}(f)\nu] = 0$ on
 415 $\partial\omega$. It follows that $[\hat{\mathbf{S}}_1(f)\nu] = -\int_0^T \chi_\omega \bar{u}^{f,\omega}(t) \bar{p}^{f,\omega}(t) dt$ which finishes the proof of
 416 (a). Part (b) is a direct consequence of part (a). \square

417 The following observation is important for our gradient algorithm that we intro-
 418 duce later on.

419 **COROLLARY 3.8.** *Let the hypotheses of Theorem 3.5 be satisfied. Assume that if*
 420 *$v \in \mathcal{U}$ then $-v \in \mathcal{U}$. Then we have*

$$421 \quad (60) \quad D\mathcal{J}_1(\omega, -f)(X) = D\mathcal{J}_1(\omega, f)(X)$$

422 for all $X \in \mathring{C}^{0,1}(\bar{\Omega}, \mathbf{R}^d)$ and $f \in H_0^1(\Omega)$.

423 *Proof.* Let $f \in H_0^1(\Omega)$ be given. From the optimality system (14) and the as-
 424 sumption that $v \in \mathcal{U}$ implies $-v \in \mathcal{U}$, we infer that $\bar{u}^{-f,\omega} = -\bar{u}^{f,\omega}$, $\bar{y}^{-f,\omega} = -\bar{y}^{f,\omega}$
 425 and $\bar{p}^{-f,\omega} = -\bar{p}^{f,\omega}$. Therefore $\mathbf{S}_1(-f) = \mathbf{S}_1(f)$ and $\mathbf{S}_0(-f) = \mathbf{S}_0(f)$ and the result
 426 follows from (45). \square

427 The following sections are devoted to the proof of Theorem 3.5(a).

428 **3.3. Sensitivity analysis of the state equation.** In this paragraph we study
 429 the sensitivity of the solution y of (1) with respect to (ω, f, u) .

430 *Perturbed state equation.* Let $X \in \mathring{C}^{0,1}(\bar{\Omega}, \mathbf{R}^d)$ be a vector field and define $T_\tau :=$
 431 $\text{id} + \tau X$. Given $u \in U$, $f \in H_0^1(\Omega)$ and $\omega \in \mathfrak{J}(\Omega)$, we consider (1) with $\omega_\tau := T_\tau(\omega)$,

$$432 \quad (61) \quad \partial_t y^{u,f,\omega_\tau} - \Delta y^{u,f,\omega_\tau} = \chi_{\omega_\tau} u \quad \text{in } \Omega \times (0, T],$$

$$433 \quad (62) \quad y^{u,f,\omega_\tau} = 0 \quad \text{on } \partial\Omega \times (0, T],$$

$$434 \quad (63) \quad y^{u,f,\omega_\tau}(0) = f \quad \text{in } \Omega.$$

436 We define the new variable

$$437 \quad (64) \quad y^{u,f,\tau} := (y^{u \circ T_\tau^{-1}, f, \omega_\tau}) \circ T_\tau.$$

438 Then since $\chi_{\omega_\tau} = \chi_\omega \circ T_\tau^{-1}$ and $\Delta f \circ T_t = \text{div}(A(t)\nabla(f \circ T_t))$, it follows from (61)-(63)
 439 that

$$440 \quad (65) \quad \partial_t y^{u,f,\tau} - \frac{1}{\xi(\tau)} \text{div}(A(\tau)\nabla y^{u,f,\tau}) = \chi_\omega u \quad \text{in } \Omega \times (0, T],$$

$$441 \quad (66) \quad y^{u,f,\tau} = 0 \quad \text{on } \partial\Omega \times (0, T],$$

$$442 \quad (67) \quad y^{u,f,\tau}(0) = f \circ T_\tau \quad \text{in } \Omega,$$

444 where

$$445 \quad A(\tau) := \det(\partial T_\tau) \partial T_\tau^{-1} \partial T_\tau^{-\top}, \quad \xi(\tau) := |\det(\partial T_\tau)|.$$

446 Equations (65)-(67) have to be understood in the variational sense, i.e., $y^{u,f,\tau} \in$
 447 $W(0, T)$ satisfying $y^{u,f,\tau}(0) = f \circ T_\tau$ and

$$448 \quad (68) \quad \int_{\Omega_\tau} \xi(\tau) \partial_t y^{u,f,\tau} \varphi + A(\tau) \nabla y^{u,f,\tau} \cdot \nabla \varphi \, dx \, dt = \int_{\Omega_\tau} \xi(\tau) \chi_\omega u \varphi \, dx \, dt$$

449

for all $\varphi \in W(0, T)$. Since $X \in \mathring{C}^{0,1}(\bar{\Omega}, \mathbf{R}^d)$, we have for fixed τ ,

$$A(\tau, \cdot), \partial_\tau A(\tau, \cdot) \in L_\infty(\Omega, \mathbf{R}^{d \times d}), \quad \xi(\tau, \cdot), \partial_\tau \xi(\tau, \cdot) \in L_\infty(\Omega).$$

450 Moreover, there are constants $c_1, c_2 > 0$, such that

$$451 \quad (69) \quad A(\tau, x)\zeta \cdot \zeta \geq c_1|\zeta|^2 \quad \text{for all } \zeta \in \mathbf{R}^d, \quad \text{for a.e } x \in \Omega, \quad \text{for all } \tau \in [0, \tau_X]$$

452 and

$$453 \quad (70) \quad \xi(\tau, x) \geq c_2 \quad \text{for a.e } x \in \Omega, \quad \text{for all } \tau \in [0, \tau_X].$$

454 *A priori estimates and continuity.*

455 LEMMA 3.9. *There is a constant $c > 0$, such that for all $(u, f, \omega) \in \mathbf{U} \times H_0^1(\Omega) \times$*
 456 *$\mathfrak{Y}(\Omega)$, and $\tau \in [0, \tau_X]$, we have*

$$457 \quad (71) \quad \begin{aligned} & \|y^{u,f,\omega_\tau}\|_{L_\infty(H^1)} + \|y^{u,f,\omega_\tau}\|_{L_2(H^2)} + \|\partial_t y^{u,f,\omega_\tau}\|_{L_2(L_2)} \\ & \leq c(\|\chi_{\omega_\tau} u\|_{L_2(L_2)} + \|f\|_{H^1}), \end{aligned}$$

458 and

$$459 \quad (72) \quad \|y^{u,f,\tau}\|_{L_\infty(H^1)} + \|\partial_t y^{u,f,\tau}\|_{L_2(L_2)} \leq c(\|\chi_\omega u\|_{L_2(L_2)} + \|f\|_{H^1}).$$

460 *Proof.* Estimate (71) is a direct consequence of (4). Let us prove (72). Recalling
 461 $y^{u,f,\tau} = y^{u \circ T_\tau^{-1}, f, \omega_\tau} \circ T_\tau$, a change of variables shows,

$$462 \quad (73) \quad \begin{aligned} & \int_{\Omega_T} |y^{u,f,\tau}|^2 + |\nabla y^{u,f,\tau}|^2 \, dx \, dt \\ & = \int_{\Omega_T} \xi^{-1}(\tau) |y^{u \circ T_\tau^{-1}, f, \omega_\tau}|^2 + A^{-1}(\tau) \nabla y^{u \circ T_\tau^{-1}, f, \omega_\tau} \cdot \nabla y^{u \circ T_\tau^{-1}, f, \omega_\tau} \, dx \, dt \\ & \leq c \int_{\Omega_T} |y^{u \circ T_\tau^{-1}, f, \omega_\tau}|^2 + |\nabla y^{u \circ T_\tau^{-1}, f, \omega_\tau}|^2 \, dx \, dt \\ & \stackrel{(71)}{\leq} c(\|\chi_{\omega_\tau} u \circ T_\tau^{-1}\|_{L_2(L_2)} + \|f\|_{H^1}) \\ & \leq C(\|\chi_\omega u\|_{L_2(L_2)} + \|f\|_{H^1}), \end{aligned}$$

463 and we further have

$$464 \quad (74) \quad \|\chi_{\omega_\tau} u \circ T_\tau^{-1}\|_{L_2(L_2)}^2 = \|\sqrt{\xi} \chi_\omega u\|_{L_2(L_2)}^2 \leq c \|\chi_\omega u\|_{L_2(L_2)}^2.$$

465 Combining (73) and (74) we obtain $\|y^{u,f,\tau}\|_{L_2(H^1)} \leq c(\|\chi_\omega u\|_{L_2(L_2)} + \|f\|_{H^1})$. In a
 466 similar fashion we can show (72). \square

467 REMARK 3.10. *An estimate for the second derivatives of $y^{u,f,\tau}$ of the form*

$$468 \quad (75) \quad \|y^{u,f,\tau}\|_{L_2(H^2)} \leq c(\|u\|_{L_2(L_2)} + \|f\|_{H^1})$$

469 *may be achieved by invoking a change of variables in the term $\|y_\tau^{u,f}\|_{L_2(H^2)}$ in (71).*
 470 *This, however, requires the vector field X to be more regular, e.g., $\mathring{C}^2(\bar{\Omega}, \mathbf{R}^d)$, and is*
 471 *not needed below.*

472 After proving a priori estimates we are ready to derive continuity results for the
 473 mapping $(u, f, \tau) \mapsto y^{u,f,\tau}$.

474 LEMMA 3.11. *For every $(\omega_1, u_1, f_1), (\omega_2, u_2, f_2) \in \mathfrak{Y}(\Omega) \times \mathbf{U} \times H_0^1(\Omega)$, we denote*
 475 *by y_1 and y_2 the corresponding solution of (61)-(63). Then there is a constant $c > 0$,*
 476 *independent of $(\omega_1, u_1, f_1), (\omega_2, u_2, f_2)$, such that*

$$477 \quad (76) \quad \begin{aligned} & \|y_1 - y_2\|_{L_\infty(H^1)} + \|y_1 - y_2\|_{L_2(H^2)} + \|\partial_t y_1 - \partial_t y_2\|_{L_2(L_2)} \\ & \leq c(\|\chi_{\omega_1} u_1 - \chi_{\omega_2} u_2\|_{L_2(L_2)} + \|f_1 - f_2\|_{H^1}). \end{aligned}$$

478 *Proof.* The difference $\tilde{y} := y_1 - y_1$ satisfies in a variational sense

$$479 \quad (77) \quad \partial_t \tilde{y} - \Delta \tilde{y} = u_1 \chi_{\omega_1} - u_2 \chi_{\omega_2} \quad \text{in } \Omega \times (0, T],$$

$$480 \quad (78) \quad \tilde{y} = 0 \quad \text{on } \partial\Omega \times (0, T],$$

$$481 \quad (79) \quad \tilde{y}(0) = f_1 - f_2 \quad \text{on } \Omega.$$

483 Hence estimate (76) follows from (4). \square

484 As an immediate consequence of Lemma 3.11 we obtain the following result.

485 LEMMA 3.12. *Let $\omega \in \mathfrak{D}(\Omega)$ be given. For all $\tau_n \in (0, \tau_X]$, $u_n, u \in \mathbf{U}$ and $f_n, f \in$*
486 *$H^1(\Omega_0)$ satisfying*

$$487 \quad (80) \quad u_n \rightharpoonup u \quad \text{in } L_2(0, T; L_2(\Omega)), \quad f_n \rightharpoonup f \quad \text{in } H_0^1(\Omega), \quad \tau_n \rightarrow 0, \quad \text{as } n \rightarrow \infty,$$

488 *we have*

$$489 \quad (81) \quad \begin{aligned} y^{u_n, f_n, \tau_n} &\overset{*}{\rightharpoonup} y^{u, f, \omega} \quad \text{in } L_\infty(0, T; H_0^1(\Omega)) \quad \text{as } n \rightarrow \infty, \\ y^{u_n, f_n, \tau_n} &\rightharpoonup y^{u, f, \omega} \quad \text{in } H^1(0, T; L_2(\Omega)) \quad \text{as } n \rightarrow \infty. \end{aligned}$$

490 *Proof.* Thanks to the apriori estimates of Lemma 3.9 there exists $y \in$
491 $L_\infty(0, T; H_0^1(\Omega)) \cap H^1(0, T; L_2(\Omega))$ and a subsequence $(y^{u_{n_k}, f_{n_k}, \tau_{n_k}})$ converging
492 weakly-star in $L_\infty(0, T; H_0^1(\Omega))$ and weakly in $H^1(0, T; L_2(\Omega))$ to y . Since $H^1(\Omega)$
493 embeds compactly into $L^2(\Omega)$ we may assume, extracting another subsequence, that
494 $f_{n_k} \rightarrow f$ in $L_2(\Omega)$ as $k \rightarrow \infty$. By definition $y_k := y^{u_{n_k}, f_{n_k}, \tau_{n_k}}$ satisfies for $k \geq 0$,

$$495 \quad (82) \quad \int_{\Omega_T} \xi(\tau_{n_k}) \partial_t y_k \varphi + A(\tau_{n_k}) \nabla y_k \cdot \nabla \varphi \, dx \, dt = \int_{\Omega_T} \xi(\tau_{n_k}) \chi_\omega u_{n_k} \varphi \, dx \, dt,$$

497 for all $\varphi \in W(0, T)$, and $y_k(0) = f_{n_k} \circ T_{\tau_{n_k}}$ on Ω . Using the weak convergence of
498 u_{n_k}, y_k stated before and the strong convergence obtained using Lemma 3.2,

$$499 \quad (83) \quad \xi(\tau_n) \rightarrow 1 \quad \text{in } L_\infty(\Omega), \quad A(\tau_n) \rightarrow I \quad \text{in } L_\infty(\Omega, \mathbf{R}^{d \times d}),$$

500 we may pass to the limit in (82) to obtain,

$$501 \quad (84) \quad \int_{\Omega_T} \partial_t y \varphi + \nabla y \cdot \nabla \varphi \, dx \, dt = \int_{\Omega_T} \chi_\omega u \varphi \, dx \, dt \quad \text{for all } \varphi \in W(0, T).$$

503 Using Lemma 3.2 we see $f_{n_k} \circ T_{\tau_{n_k}} \rightarrow f$ in $L_2(\Omega)$ as $k \rightarrow \infty$, and therefore $y(0) = f$.
504 Since the previous equation with $y(0) = f$ admits a unique solution we conclude that
505 $y = y^{u, f, \omega}$. As a consequence of the uniqueness of the limit, the whole sequence
506 y^{u_n, f_n, τ_n} converges to $y^{u, f, \omega}$. This finishes the proof. \square

507 **3.4. Sensitivity of minimisers and maximisers.** Let us denote for $(\tau, f) \in$
508 $[0, \tau_X] \times K$ the minimiser of $u \mapsto J(\omega_\tau, u \circ T_\tau^{-1}, f)$, by \bar{u}^{f_n, τ_n} .

509 LEMMA 3.13. *For every null-sequence (τ_n) in $[0, \tau_X]$ and every sequence (f_n) in*
510 *K converging weakly (in $H_0^1(\Omega)$) to $f \in K$, we have*

$$511 \quad (85) \quad \bar{u}^{f_n, \tau_n} \rightarrow \bar{u}^{f, \omega} \quad \text{in } L_2(0, T; L_2(\Omega)) \quad \text{as } n \rightarrow \infty.$$

512 *Proof.* We set $\omega_n := \omega_{\tau_n}$. By definition we have $\bar{u}^{f_n, \tau_n} = \bar{u}^{f_n, \omega_{\tau_n}} \circ T_{\tau_n}$. From
513 Lemma 2.3 we know that $\bar{u}^{f_n, \omega_{\tau_n}}$ converges to $\bar{u}^{f_n, \omega}$ in $L_2(0, T; L_2(\Omega))$. Therefore
514 according to Lemma 3.2 also $\bar{u}^{f_n, \omega_{\tau_n}} \circ T_{\tau_n}$ converges in $L_2(0, T; L_2(\Omega))$ to $\bar{u}^{f_n, \omega}$. This
515 finishes the proof. \square

516 LEMMA 3.14. For every null-sequence (τ_n) in $[0, \tau_X]$ and every sequence (f_n) ,
 517 $f_n \in \mathfrak{X}_2(\omega_{\tau_n})$, there is a subsequence (f_{n_k}) and $f \in \mathfrak{X}_2(\omega)$, such that $f_{n_k} \rightharpoonup f$ in
 518 $H_0^1(\Omega)$ as $k \rightarrow \infty$.

519 *Proof.* We proceed similarly as in the proof of Lemma 3.13. Let $\tau \in [0, \tau_X]$ and
 520 $v \in U$ be given. We obtain for all $f \in K$,

$$521 \quad (86) \quad J(\omega_\tau, u^{f, \tau} \circ T_\tau^{-1}, f) = \inf_{u \in U} J(\omega_\tau, u \circ T_\tau^{-1}, f) \leq J(\omega_\tau, v \circ T_\tau^{-1}, f).$$

522 Let (\bar{f}_n) be an arbitrary sequence with $\bar{f}_n \in \mathfrak{X}_2(\omega_{\tau_n})$. Since $\|\bar{f}_n\|_{H_0^1(\Omega)} \leq 1$ for all
 523 $n \geq 0$, there is a subsequence (\bar{f}_{n_k}) and a function $\bar{f} \in K$, such that $\bar{f}_{n_k} \rightharpoonup \bar{f}$ in $H_0^1(\Omega)$
 524 as $k \rightarrow \infty$ and $\|\bar{f}\|_{H_0^1(\Omega)} \leq 1$. Thanks to Lemma 3.13 the sequence (\bar{u}_k) defined by
 525 $\bar{u}_k := \bar{u}^{\bar{f}_{n_k}, \tau_{n_k}}$ converges to $\bar{u}^{\bar{f}, \omega}$ in $L_2(0, T; L_2(\Omega))$. Moreover, Lemma 3.12 also shows
 526 that $y^{\bar{u}_k, \bar{f}_{n_k}, \tau_{n_k}} \rightarrow y^{\bar{u}^{\bar{f}, \omega}, \bar{f}, \omega}$ in $L_2(0, T; L_2(\Omega))$. By definition for all $k \geq 0$ and $f \in K$,

$$\begin{aligned} & \int_{\Omega_T} |y^{\bar{u}^{\bar{f}, \tau_{n_k}}, f, \tau_{n_k}}(t)|^2 + \gamma |\bar{u}^{f, \tau_{n_k}}(t)|^2 dx dt \\ 527 \quad (87) \quad & \leq \sup_{\substack{f \in K \\ \|f\|_{H_0^1(\Omega)} \leq 1}} \int_{\Omega_T} |y^{\bar{u}^{\bar{f}, \tau_{n_k}}, f, \tau_{n_k}}(t)|^2 + \gamma |\bar{u}^{f, \tau_{n_k}}(t)|^2 dx dt \\ & = \int_{\Omega_T} |y^{\bar{u}_k, \bar{f}_{n_k}, \tau_{n_k}}(t)|^2 + \gamma |\bar{u}_k(t)|^2 dx dt \end{aligned}$$

528 and therefore passing to the limit $k \rightarrow \infty$ yields, for all $f \in K$,

$$529 \quad (88) \quad \int_{\Omega_T} |y^{\bar{u}^{\bar{f}, \omega}, f, \omega}(t)|^2 + \gamma |\bar{u}^{f, \omega}(t)|^2 dx dt \leq \int_{\Omega_T} |y^{\bar{u}^{\bar{f}, \omega}, \bar{f}, \omega}(t)|^2 + \gamma |\bar{u}^{\bar{f}, \omega}(t)|^2 dx dt.$$

530 This shows that $f \in \mathfrak{X}_2(\omega)$ and finishes the proof. \square

531 **3.5. Averaged adjoint equation and Lagrangian.** For fixed $\tau \in [0, \tau_X]$ the
 532 mapping $\varphi \mapsto T_\tau^{-1} \circ \varphi$ is an isomorphism on U , therefore,

$$533 \quad (89) \quad \min_{u \in U} J(\omega_\tau, u, f) = \min_{u \in U} J(\omega_\tau, u \circ T_\tau^{-1}, f).$$

534 Hence a change of variables shows,

$$\begin{aligned} 535 \quad (90) \quad \inf_{u \in U} J(\omega_\tau, u, f) &= \inf_{u \in U} \int_0^T \|y^{u, f, \omega_\tau}(t)\|_{L_2(\Omega)}^2 + \gamma \|u(t)\|_{L_2(\Omega)}^2 dt \\ &\stackrel{(89)}{=} \inf_{u \in U} \int_{\Omega_T} \xi(\tau) (|y^{u, f, \tau}(t)|^2 + \gamma |u(t)|^2) dx dt. \end{aligned}$$

536 Introduce for every quadruple $(u, f, y, p) \in U \times K \times W(0, T) \times W(0, T)$ and for every
 537 $\tau \in [0, \tau_X]$ the parametrised Lagrangian

$$\begin{aligned} 538 \quad (91) \quad \tilde{G}(\tau, u, f, y, p) &:= \int_{\Omega_T} \xi(\tau) (|y|^2 + \gamma |u|^2) dx dt \\ &+ \int_{\Omega_T} \xi(\tau) \partial_t y p dx dt + A(\tau) \nabla y \cdot \nabla p dx dt \\ &- \int_{\Omega_T} \xi(\tau) u \chi_\omega p dx dt + \int_\Omega \xi(\tau) (y(0) - f \circ T_\tau) p(0) dx. \end{aligned}$$

539 DEFINITION 3.15. Given $(u, f) \in U \times K$, and $\tau \in [0, \tau_X]$, the averaged adjoint
540 state $p^{u,f,\tau} \in W(0, T)$ is the solution of averaged adjoint equation

$$541 \quad (92) \quad \int_0^1 \partial_y \tilde{G}(\tau, u, f, sy^{u,f,\tau} + (1-s)y^{u,f,\omega}, p^{u,f,\tau})(\varphi) ds = 0 \quad \text{for all } \varphi \in W(0, T).$$

542 REMARK 3.16. The averaged adjoint state $p^{u,f,\tau}$ in our special case only depends
543 on u and f through the state $y^{u,f,\tau}$.

544 It is evident that (92) is equivalent to

$$(93) \quad \int_{\Omega_T} \xi(\tau) \partial_t \varphi p^{u,f,\tau} + A(\tau) \nabla \varphi \cdot \nabla p^{u,f,\tau} dx dt + \int_{\Omega} \xi(\tau) p^{u,f,\tau}(0) \varphi(0) dx$$

$$545 \quad = - \int_{\Omega_T} \xi(\tau) (y^{u,f,\tau} + y^{u,f,\omega}) \varphi dx dt$$

546 for all $\varphi \in W(0, T)$, or equivalently after partial integration in time

$$(94) \quad \int_{\Omega_T} -\xi(\tau) \varphi \partial_t p^{u,f,\tau} + A(\tau) \nabla \varphi \cdot \nabla p^{u,f,\tau} dx dt = - \int_{\Omega_T} \xi(\tau) (y^{u,f,\tau} + y^{u,f,\omega}) \varphi dx dt$$

548 for all $\varphi \in W(0, T)$, and $p^{u,f,\tau}(T) = 0$. This is a backward in time linear parabolic
549 equation with terminal condition zero.

550 **3.6. Differentiability of max-min functions.** Before we can pass to the proof
551 of Theorem 3.5 we need to address a Danskin type theorem on the differentiability of
552 max-min functions.

553 Let \mathfrak{U} and \mathfrak{Y} be two nonempty sets and let $G : [0, \tau] \times \mathfrak{U} \times \mathfrak{Y} \rightarrow \mathbf{R}$ be a function,
554 $\tau > 0$. Introduce the function $g : [0, \tau] \rightarrow \mathbf{R}$,

$$555 \quad (95) \quad g(t) := \sup_{y \in \mathfrak{Y}} \inf_{x \in \mathfrak{U}} G(t, x, y)$$

556 and let $\ell : [0, \tau] \rightarrow \mathbf{R}$ be any function such that $\ell(t) > 0$ for $t \in (0, \tau]$ and $\ell(0) = 0$.
557 We are interested in sufficient conditions that guarantee that the limit

$$558 \quad (96) \quad \frac{d}{d\ell} g(0^+) := \lim_{t \searrow 0^+} \frac{g(t) - g(0)}{\ell(t)}$$

559 exists. Moreover we define for $t \in [0, \tau]$,

$$560 \quad (97) \quad \mathfrak{Y}(t) := \{y^t \in \mathfrak{Y} : \sup_{y \in \mathfrak{Y}} \inf_{x \in \mathfrak{U}} G(t, x, y) = \inf_{x \in \mathfrak{U}} G(t, x, y^t)\}.$$

561 LEMMA 3.17. Let the following hypotheses be satisfied.

562 (A0) For all $y \in \mathfrak{Y}$ and $t \in [0, \tau]$ the minimisation problem

$$563 \quad (98) \quad \inf_{x \in \mathfrak{U}} G(t, x, y)$$

564 admits a unique solution and we denote this solution by $x^{t,y}$.

565 (A1) For all t in $[0, \tau]$ the set $\mathfrak{Y}(t)$ is nonempty.

566 (A2) *The limits*

$$567 \quad (99) \quad \lim_{t \searrow 0} \frac{G(t, x^{t,y}, y) - G(0, x^{t,y}, y)}{\ell(t)}$$

568 *and*

$$569 \quad (100) \quad \lim_{t \searrow 0} \frac{G(t, x^{0,y}, y) - G(0, x^{0,y}, y)}{\ell(t)}$$

570 *exist for all $y \in \mathfrak{A}$ and they are equal. We denote the limit by*
 571 $\partial_\ell G(0^+, x^{0,y}, y)$.

572 (A3) *For all real null-sequences (t_n) in $(0, \tau]$ and all sequences y^{t_n} in $\mathfrak{B}(t_n)$, there*
 573 *exists a subsequence (t_{n_k}) of (t_n) , and $(y^{t_{n_k}})$ of (y^{t_n}) , and y^0 in $\mathfrak{B}(0)$, such*
 574 *that*

$$575 \quad (101) \quad \lim_{k \rightarrow \infty} \frac{G(t_{n_k}, x^{t_{n_k}, y^{t_{n_k}}}, y^{t_{n_k}}) - G(0, x^{t_{n_k}, y^{t_{n_k}}}, y^{t_{n_k}})}{\ell(t_{n_k})} = \partial_\ell G(0^+, x^{0, y^0}, y^0)$$

576 *and*

$$577 \quad (102) \quad \lim_{k \rightarrow \infty} \frac{G(t_{n_k}, x^{0, y^{t_{n_k}}}, y^{t_{n_k}}) - G(0, x^{0, y^{t_{n_k}}}, y^{t_{n_k}})}{\ell(t_{n_k})} = \partial_\ell G(0^+, x^{0, y^0}, y^0).$$

578 *Then we have*

$$579 \quad (103) \quad \frac{d}{d\ell} g(t)|_{t=0^+} = \max_{y \in \mathfrak{B}(0)} \partial_\ell G(0^+, x^{0,y}, y).$$

580 In this section we apply the previous results for $\ell(t) = t$, and in the following one
 581 for $\ell(t) = |B_t(\eta_0)|$, $\eta_0 \in \mathbf{R}^d$. For the sake of completeness we give a proof in the
 582 appendix; see [8].

583 **3.7. Proof of Theorem 3.5.** The following is a direct consequence of (94) and
 584 Lemma 3.12.

585 LEMMA 3.18. *For all sequences $\tau_n \in (0, \tau_X]$, $u_n, u \in \mathbf{U}$ and $f_n, f \in K$, such that*

$$586 \quad (104) \quad u_n \rightharpoonup u \quad \text{in } \mathbf{U}, \quad f_n \rightharpoonup f \quad \text{in } H_0^1(\Omega), \quad \tau_n \rightarrow 0, \quad \text{as } n \rightarrow \infty,$$

587 *we have*

$$588 \quad (105) \quad \begin{aligned} p^{u_n, f_n, \tau_n} &\rightharpoonup p^{u, f, \omega} && \text{in } L_2(0, T; H_0^1(\Omega)) && \text{as } n \rightarrow \infty, \\ p^{u_n, f_n, \tau_n} &\rightharpoonup p^{u, f, \omega} && \text{in } H^1(0, T; L_2(\Omega)) && \text{as } n \rightarrow \infty, \end{aligned}$$

589 *where $p^{u, f, \omega} \in Z(0, T)$ solves the adjoint equation*

$$590 \quad (106) \quad \int_{\Omega_T} -\varphi \partial_t p^{u, f, \omega} \, dx \, dt + \int_{\Omega_T} \nabla \varphi \cdot \nabla p^{u, f, \omega} \, dx \, dt = - \int_{\Omega_T} 2y^{u, f, \omega} \varphi \, dx \, dt$$

591 *for all $\varphi \in W(0, T)$, and $p^{u, f, \omega}(T) = 0$ a.e. on Ω .*

592 Now we have gathered all the ingredients to complete the proof of Theorem 3.5(a)
 593 on page 9.

594 **Proof of Theorem 3.5(a)** Using the fundamental theorem of calculus we obtain for
595 all $\tau \in [0, \tau_X]$,

$$(107) \quad \begin{aligned} & \tilde{G}(\tau, u, f, y^{u,f,\tau}, p^{u,f,\tau}) - \tilde{G}(\tau, u, f, y^{u,f,\omega}, p^{u,f,\omega}) \\ &= \int_0^1 \partial_y \tilde{G}(\tau, u, f, sy^{u,f,\tau} + (1-s)y^{u,f,\omega}, p^{u,f,\tau})(y^{u,f,\tau} - y^{u,f,\omega}) ds = 0, \end{aligned}$$

597 where in the last step we used the averaged adjoint equation (94). In addition we
598 have $J(\omega_\tau, u \circ T_\tau^{-1}, f) = \tilde{G}(\tau, u, f, y^{u,f,\omega}, p^{u,f,\tau})$, which together with (107) gives

$$599 \quad (108) \quad J(\omega_\tau, u \circ T_\tau^{-1}, f) = \tilde{G}(\tau, u, f, y^{u,f,\omega}, p^{u,f,\tau}).$$

600 As a consequence we obtain

$$601 \quad (109) \quad \mathcal{J}_1(\omega_\tau, f) = \inf_{u \in \mathcal{U}} \tilde{G}(\tau, u, f, y^{u,f,\omega}, p^{u,f,\tau}).$$

602 We apply Lemma 3.17 with $\ell(t) := t$,

$$603 \quad (110) \quad G(\tau, u, f) := \tilde{G}(\tau, u, f, y^{u,f,\omega}, p^{u,f,\tau}),$$

604 $\mathfrak{U} = \mathcal{U}$, and $\mathfrak{V} = \{f \in K : \|f\|_{H_0^1(\Omega)} \leq 1\}$.

605 Since the minimization problem (90) admits a unique solution, Assumption (A0) is
606 satisfied. A minor change in the proof of Lemma 2.4 to accommodate the reparametri-
607 zation of the domain ω shows that (A1) is satisfied as well.

608 Let (τ_n) be an arbitrary null-sequence and let (f_n) be a sequence in K converging
609 weakly in $H_0^1(\Omega)$ to $f \in K$, and let us set $\bar{u}_n := \bar{u}^{f_n, \tau_n}$. Thanks to Lemma 3.13 we
610 have that \bar{u}_n converges strongly in $L_2(0, T; L_2(\Omega))$ to $\bar{u}^{f, \omega}$. Moreover Lemma 3.18
611 implies

$$612 \quad (111) \quad \begin{aligned} p^{\bar{u}_n, f_n, \tau_n} &\rightarrow p^{\bar{u}^{f, \omega}, f, \omega} && \text{in } L_2(0, T; H_0^1(\Omega)) && \text{as } n \rightarrow \infty, \\ p^{\bar{u}_n, f_n, \tau_n} &\rightarrow p^{\bar{u}^{f, \omega}, f, \omega} && \text{in } H^1(0, T; L_2(\Omega)) && \text{as } n \rightarrow \infty. \end{aligned}$$

613 Using Lemma 3.7 we see that

$$614 \quad (112) \quad \frac{A(\tau_n) - I}{\tau_n} \rightarrow \operatorname{div}(X) - \partial X - \partial X^\top \quad \text{in } L_\infty(\Omega, \mathbf{R}^{d \times d}) \quad \text{as } n \rightarrow \infty,$$

615 and

$$616 \quad (113) \quad \frac{\xi(\tau_n) - 1}{\tau_n} \rightarrow \operatorname{div}(X) \quad \text{in } L_\infty(\Omega) \quad \text{as } n \rightarrow \infty.$$

617 Therefore we get

$$\begin{aligned}
& \frac{G(\tau_n, \bar{u}_n, f_n) - G(0, \bar{u}_n, f_n)}{\tau_n} \\
&= \frac{\tilde{G}(\tau_n, \bar{u}_n, f_n, y^{\bar{u}_n, f_n, \omega}, p^{\bar{u}_n, f_n, \tau_n}) - \tilde{G}(0, \bar{u}_n, f_n, y^{\bar{u}_n, f_n, \omega}, p^{\bar{u}_n, f_n, \tau_n})}{\tau_n} \\
&= \int_{\Omega_T} \frac{\xi(\tau_n) - 1}{\tau} (|y^{\bar{u}_n, f_n, \omega}|^2 + \gamma |\bar{u}_n|^2) \, dx dt \\
618 \quad (114) \quad &+ \int_{\Omega_T} \frac{\xi(\tau_n) - 1}{\tau} \partial_t y^{\bar{u}_n, f_n, \omega} p^{\bar{u}_n, f_n, \tau_n} \, dx dt \\
&+ \int_{\Omega_T} \frac{A(\tau_n) - I}{\tau_n} \nabla y^{\bar{u}_n, f_n, \omega} \cdot \nabla p^{\bar{u}_n, f_n, \tau_n} \, dx dt \\
&- \int_{\Omega_T} \frac{\xi(\tau_n) - 1}{\tau} \bar{u}_n \chi_\omega p^{\bar{u}_n, f_n, \tau_n} \, dx dt \\
&+ \int_{\Omega} \left(\frac{\xi(\tau_n) - 1}{\tau_n} (y^{\bar{u}_n, f_n, \omega}(0) - f_n \circ T_{\tau_n}) - \frac{f_n \circ T_{\tau_n} - f_n}{\tau_n} \right) p^{\bar{u}_n, f_n, \tau_n}(0) \, dx
\end{aligned}$$

619 and using Lemma 3.2 and (111), we see that the right hand side tends to

$$\begin{aligned}
(115) \quad & \int_{\Omega_T} \operatorname{div}(X) (|\bar{y}^{f, \omega}|^2 + \gamma |\bar{u}^{f, \omega}|^2 + \partial_t \bar{y}^{f, \omega} \bar{p}^{f, \omega} + \nabla \bar{y}^{f, \omega} \cdot \nabla \bar{p}^{f, \omega} - \bar{u}^{f, \omega} \bar{p}^{f, \omega} \chi_\omega) \, dx dt \\
620 \quad & - \int_{\Omega_T} \partial X \nabla \bar{y}^{f, \omega} \cdot \nabla \bar{p}^{f, \omega} + \partial X \nabla \bar{p}^{f, \omega} \cdot \nabla \bar{y}^{f, \omega} + \frac{1}{T} \nabla f \cdot X \bar{p}^{f, \omega}(0) \, dx dt.
\end{aligned}$$

621 Partial integration in time yields

$$(116) \quad \int_{\Omega_T} \bar{p}^{f, \omega} \partial_t \bar{y}^{f, \omega} \operatorname{div}(X) \, dx dt = - \int_{\Omega_T} \partial_t \bar{p}^{f, \omega} \bar{y}^{f, \omega} \operatorname{div}(X) \, dx dt - \int_{\Omega} \operatorname{div}(X) f \bar{p}^{f, \omega}(0) \, dx,$$

623 where we used $\bar{y}^{f, \omega}(0) = f$ and $\bar{p}^{f, \omega}(T) = 0$. As a result, inserting (116) into (115),
624 we see that (115) can be written as

$$(117) \quad \int_{\Omega_T} \mathbf{S}_1(\bar{y}^{f, \omega}, \bar{p}^{f, \omega}, u^{f, \omega}) : \partial X + \mathbf{S}_0 \cdot X \, dx dt$$

626 with $\mathbf{S}_1, \mathbf{S}_2$ being given by (41). Hence we obtain

$$(118) \quad \lim_{n \rightarrow \infty} \frac{G(\tau_n, \bar{u}_n, f_n) - G(0, \bar{u}_n, f_n)}{\tau_n} = \int_{\Omega_T} \mathbf{S}_1(\bar{y}^{f, \omega}, \bar{p}^{f, \omega}, u^{f, \omega}) : \partial X + \mathbf{S}_0 \cdot X \, dx dt.$$

628 Next let $\bar{u}_{n,0} := \bar{u}^{f_n, 0}$. Then we can show in as similar manner as (118) that

$$(119) \quad \lim_{n \rightarrow \infty} \frac{G(\tau_n, \bar{u}_{n,0}, f_n) - G(0, \bar{u}_{n,0}, f_n)}{\tau_n} = \int_{\Omega_T} \mathbf{S}_1(\bar{y}^{f, \omega}, \bar{p}^{f, \omega}, u^{f, \omega}) : \partial X + \mathbf{S}_0 \cdot X \, dx dt.$$

630 Hence choosing (f_n) to be a constant sequence we see that (A2) is satisfied.

631 But also (A3) is satisfied since according to Lemma 3.14 we find for every null-
632 sequence (τ_n) in $[0, \tau_X]$ and every sequence (f_n) , $f_n \in \mathfrak{X}_2(\omega_{\tau_n})$, a subsequence (f_{n_k})

633 and $f \in \mathfrak{X}_2(\omega)$, such that $f_{n_k} \rightharpoonup f$ in $H_0^1(\Omega)$ as $k \rightarrow \infty$. Now we use (118) and
 634 (119) with f_n replaced by this choice of f_{n_k} , and conclude that (A3) holds. Thus all
 635 requirements of Lemma 3.17 are satisfied and this ends the proof of Theorem 3.5(a).

636 **4. Topological derivative.** In this section we will derive the topological deriva-
 637 tive of the shape functions \mathcal{J}_1 and \mathcal{J}_2 introduced in (7) and (8), respectively. The
 638 topological derivative, introduced in [22], allows to predict the position where small
 639 holes in the shape should be inserted in order to achieve a decrease of the shape
 640 function.

641 **4.1. Definition of topological derivative.** We begin by introducing the so-
 642 called topological derivative. For more details we refer to [20].

643 **DEFINITION 4.1** (Topological derivative). *The topological derivative of a shape*
 644 *functional $J : \mathfrak{Y}(\Omega) \rightarrow \mathbf{R}$ at $\omega \in \mathfrak{Y}(\Omega)$ in the point $\eta_0 \in \Omega \setminus \partial\omega$ is defined by*

$$645 \quad (120) \quad \mathcal{T}J(\omega)(\eta_0) = \begin{cases} \lim_{\epsilon \searrow 0} \frac{J(\omega \setminus \bar{B}_\epsilon(\eta_0)) - J(\omega)}{|B_\epsilon(\eta_0)|} & \text{if } \eta_0 \in \omega, \\ \lim_{\epsilon \searrow 0} \frac{J(\omega \cup B_\epsilon(\eta_0)) - J(\omega)}{|B_\epsilon(\eta_0)|} & \text{if } \eta_0 \in \Omega \setminus \bar{\omega}. \end{cases}$$

646 **4.2. Second main result: topological derivative of \mathcal{J}_2 .** Given $\omega \in \mathfrak{Y}(\Omega)$
 647 we set $\omega_\epsilon := \Omega \setminus \bar{B}(\eta_0)$ if $\eta_0 \in \omega$ and $\omega_\epsilon := \omega \cup B_\epsilon(\eta_0)$ if $\eta_0 \in \Omega \setminus \bar{\omega}$. Denote by $\bar{u}^{f, \omega_\epsilon}$
 648 the minimiser of the right hand side of (7) with $\omega = \omega_\epsilon$.

649 **ASSUMPTION 4.2.** *Let $\delta > 0$ be so small that $\bar{B}_\delta(\eta_0) \Subset \Omega$. We assume that for all*
 650 *$(f, \omega) \in V \times \mathfrak{Y}(\Omega)$ we have $\bar{u}^{f, \omega} \in C(\bar{B}_\delta(\eta_0))$. Furthermore we assume that for every*
 651 *sequence (ω_n) in $\mathfrak{Y}(\Omega)$ converging to $\omega \in \mathfrak{Y}(\Omega)$ and every weakly converging sequence*
 652 *$f_n \rightharpoonup f$ in V we have*

$$653 \quad (121) \quad \lim_{n \rightarrow \infty} \|\bar{u}^{f_n, \omega_n} - \bar{u}^{f, \omega}\|_{L_1(0, T; C(\bar{B}_\delta(\eta_0)))} = 0.$$

654 **REMARK 4.3.** *Lemmas 2.3, 2.2 show that Assumption 4.2 is satisfied in case \mathcal{U}*
 655 *is equal to $L_2(\Omega)$ or \mathbf{R} . Indeed in case $\mathcal{U} = \mathbf{R}$ we have shown in Remark 2.1, (b) that*
 656 *$2\gamma \bar{u}^{\omega, f}(t) = \int_\omega \bar{p}^{f, \omega}(t, x) dx$, so that $\bar{u}^{\omega, f}$ is independent of space and Assumption 4.2*
 657 *is satisfied thanks to Lemma 2.3. In case $\mathcal{U} = L_2(\Omega)$ Remark 2.1, (a) shows that*
 658 *$2\gamma \bar{u}^{\omega, f} = \bar{p}^{f, \omega}$. In Lemma 4.7 below we show that $(f, \omega) \mapsto \bar{p}^{f, \omega} : V \times \mathfrak{Y}(\Omega) \rightarrow$*
 659 *$C([0, T] \times \bar{B}_\delta(\eta_0))$ is continuous for small $\delta > 0$, when V is equipped with the weak*
 660 *convergence we also see that in this case Assumption 4.2 is satisfied.*

661 For $\omega \in \mathfrak{Y}(\Omega)$ and $f \in K$, we set $\bar{y}^{f, \omega} := y^{\bar{u}^{\omega, f}, f, \omega}$ and $\bar{p}^{f, \omega} := p^{\bar{u}^{\omega, f}, f, \omega}$. The
 662 main result that we are going to establish reads as follows.

663 **THEOREM 4.4.** *Let $\omega \in \mathfrak{Y}(\Omega)$ be open. Let Assumption 4.2 be satisfied at $\eta_0 \in$*
 664 *$\Omega \setminus \partial\omega$. Then the topological derivative of $\omega \mapsto \mathcal{J}_2(\omega)$ at ω in η_0 is given by*

$$665 \quad (122) \quad \mathcal{T}\mathcal{J}_2(\omega)(\eta_0) = \max_{f \in \mathfrak{X}_2(\omega)} \begin{cases} -\int_0^T \bar{u}^{f, \omega}(\eta_0, s) \bar{p}^{f, \omega}(\eta_0, s) ds & \text{if } \eta_0 \in \omega, \\ \int_0^T \bar{u}^{f, \omega}(\eta_0, s) \bar{p}^{f, \omega}(\eta_0, s) ds & \text{if } \eta_0 \in \Omega \setminus \bar{\omega}, \end{cases}$$

666 where the adjoint $\bar{p}^{f, \omega}$ belongs to $C([0, T] \times B_\delta(\eta_0))$ and satisfies

$$667 \quad (123) \quad \partial_t \bar{p}^{f, \omega} - \Delta \bar{p}^{f, \omega} = -2\bar{y}^{f, \omega} \quad \text{in } \Omega \times (0, T],$$

$$668 \quad (124) \quad \bar{p}^{f, \omega} = 0 \quad \text{on } \partial\Omega \times (0, T],$$

$$669 \quad (125) \quad \bar{p}^{f, \omega}(T) = 0 \quad \text{in } \Omega.$$

671 COROLLARY 4.5. *Let the assumptions of the previous theorem be satisfied. Let*
 672 *$f \in V$ be given. Then topological derivative of $\omega \mapsto \mathcal{J}_1(\omega, f)$ at ω in η_0 is given by*

$$673 \quad (126) \quad \mathcal{T} \mathcal{J}_1(\omega, f)(\eta_0) = \begin{cases} -\int_0^T \bar{u}^{f,\omega}(x_0, s) \bar{p}^{f,\omega}(\eta_0, s) ds & \text{if } \eta_0 \in \omega, \\ \int_0^T \bar{u}^{f,\omega}(x_0, s) \bar{p}^{f,\omega}(\eta_0, s) ds & \text{if } \eta_0 \in \Omega \setminus \bar{\omega}, \end{cases}$$

674 *where $\bar{p}^{f,\omega}$ solves the adjoint equation (123).*

675 *Proof.* For the same arguments as in proof of Theorem 3.5 we may assume that
 676 $\bar{f} \in K$ with $\|\bar{f}\|_V \leq 1$. Setting $K := \{\bar{f}\}$ we obtain for all $\omega \in \mathfrak{Y}(\Omega)$,

$$677 \quad (127) \quad \mathcal{J}_2(\omega) = \max_{\substack{f \in K, \\ \|f\|_V \leq 1}} \mathcal{J}_1(\omega, f) = \mathcal{J}_1(\omega, \bar{f})$$

678 and hence the result follows from Theorem 3.5 since $\mathfrak{X}_2(\omega) = \{\bar{f}\}$ is a singleton. \square

679 COROLLARY 4.6. *Let the hypotheses of Theorem 4.4 be satisfied. Assume that if*
 680 *$v \in \mathcal{U}$ then $-v \in \mathcal{U}$. Then we have*

$$681 \quad (128) \quad \mathcal{T} \mathcal{J}_1(\omega, -f)(\eta_0) = \mathcal{T} \mathcal{J}_1(\omega, f)(\eta_0)$$

682 *for all $\eta_0 \in \Omega \setminus \partial\omega$ and $f \in V$.*

683 *Proof.* Let $f \in V$ be given. From the optimality system (14) and the assumption
 684 that $v \in \mathcal{U}$ implies $-v \in \mathcal{U}$, we infer that $\bar{u}^{-f,\omega} = -\bar{u}^{f,\omega}$, $\bar{y}^{-f,\omega} = -\bar{y}^{f,\omega}$ and
 685 $\bar{p}^{-f,\omega} = -\bar{p}^{f,\omega}$. Now the result follows from (126). \square

686 **4.3. Averaged adjoint equation and Lagrangian.** Throughout this section
 687 we fix an open set $\omega \in \mathfrak{Y}(\Omega)$ and pick $\eta_0 \in \omega$. The case $\eta_0 \in \Omega \setminus \bar{\omega}$ is treated similarly.
 688 Let us define $\omega_\epsilon := \omega \setminus \bar{B}_\epsilon(\eta_0)$, $\epsilon > 0$.

689 For every quadruple $(u, f, y, p) \in U \times K \times W(0, T) \times W(0, T)$ and every $\epsilon \geq 0$ we
 690 define the parametrised Lagrangian,

$$691 \quad (129) \quad \begin{aligned} \tilde{G}(\epsilon, u, f, y, p) := & \int_{\Omega_T} y^2 + \gamma u^2 dx dt + \int_{\Omega_T} \partial_t y p + \nabla y \cdot \nabla p dx dt \\ & - \int_{\Omega_T} \chi_{\omega_\epsilon} u p dx dt + \int_{\Omega} (y(0) - f \circ T_\tau) p(0) dx. \end{aligned}$$

692 We denote by $y^{u,f,\epsilon} \in W(0, T)$ the solution of the state equation (1) with $\chi = \chi_{\omega_\epsilon}$ in
 693 (1a). Then, similarly to (92), we introduce the averaged adjoint: find $p^{u,f,\epsilon} \in W(0, T)$,
 694 such that

$$695 \quad (130) \quad \int_0^1 \partial_y \tilde{G}(\epsilon, u, f, \sigma y^{u,f,\epsilon} + (1 - \sigma) y^u, p^{u,f,\epsilon})(\varphi) d\sigma = 0 \quad \text{for all } \varphi \in W(0, T)$$

696 or equivalently after partial integration in time, $p^{u,f,\epsilon}(T) = 0$ and

$$697 \quad (131) \quad \int_{\Omega_T} -\varphi \partial_t p^{u,f,\epsilon} + \nabla \varphi \cdot \nabla p^{u,f,\epsilon} dx dt = - \int_{\Omega_T} (y^{u,f,\epsilon} + y^{u,f}) \varphi dx dt$$

698 for all $\varphi \in W(0, T)$.

699 **4.4. Proof of Theorem 4.4.**

700 LEMMA 4.7. *Let $\delta > 0$ be such that $\bar{B}_\delta(\eta_0) \Subset \Omega$. For all sequences $\epsilon_n \in (0, 1]$,*
 701 *$u_n, u \in \mathbf{U}$ and $f_n, f \in K$, such that*

$$702 \quad (132) \quad u_n \rightharpoonup u \quad \text{in } \mathbf{U}, \quad f_n \rightharpoonup f \quad \text{in } V, \quad \epsilon_n \rightarrow 0, \quad \text{as } n \rightarrow \infty,$$

703 *we have*

$$704 \quad (133) \quad \begin{aligned} p^{u_n, f_n, \epsilon_n} &\rightarrow p^{u, f, \omega} && \text{in } L_2(0, T; H_0^1(\Omega)) && \text{as } n \rightarrow \infty, \\ p^{u_n, f_n, \epsilon_n} &\rightarrow p^{u, f, \omega} && \text{in } H^1(0, T; L_2(\Omega)) && \text{as } n \rightarrow \infty. \end{aligned}$$

705 *Moreover there is a subsequence $(p^{u_{n_k}, f_{n_k}, \epsilon_{n_k}})$, such that*

$$706 \quad (134) \quad p^{u_{n_k}, f_{n_k}, \epsilon_{n_k}} \rightarrow p^{u, f, \omega} \quad \text{in } C([0, T] \times \bar{B}_\delta(\eta_0)) \quad \text{as } n \rightarrow \infty.$$

707 *Proof.* The first two statements follow by a similar arguments as used in Lemma 3.18. ■

708 To prove the third we have by interior regularity of parabolic equations that

$$709 \quad (135) \quad p^{u, f, \epsilon} \in \tilde{Z}(0, T) := L_2(0, T; H^4(B_\delta(\eta_0))) \cap H^1(0, T; H_0^1(B_\delta(\eta_0))) \cap H^2(0, T; L_2(B_\delta(\eta_0))) \blacksquare$$

710 and we have the apriori bound

$$711 \quad (136) \quad \begin{aligned} \sum_{k=0}^2 \left\| \left(\frac{d}{dt} \right)^k p^{u, f, \epsilon} \right\|_{L_2(0, T; H^{4-2k}(B_\delta(\eta_0)))} \\ \leq c(\|y^{u, f, \epsilon} + y^{u, f}\|_{L_2(H^2)} + \left\| \frac{d}{dt}(y^{u, f, \epsilon} + y^{u, f}) \right\|_{L_2(L_2)}), \end{aligned}$$

712 see e.g. [10, p.365-367, Thm.6]. Hence (134) follows since the space $\tilde{Z}(0, T)$ embeds
 713 compactly into $C([0, T] \times \bar{B}_\delta(\eta_0))$. □

714 **Proof of Theorem 4.4** Proceeding as in the proof of Theorem 3.5 we obtain using
 715 the averaged adjoint equation,

$$716 \quad (137) \quad J(\epsilon, u, f) = \tilde{G}(\epsilon, u, f, y^{u, f, \omega}, p^{u, f, \epsilon})$$

717 for $(\epsilon, u, f) \in [0, 1] \times \mathbf{U} \times K$, where \tilde{G} is defined in (129). Hence to prove Theorem 4.4
 718 it suffices to apply Lemma 3.17 with

$$719 \quad (138) \quad G(\epsilon, u, f) := \tilde{G}(\epsilon, u, f, y^{u, f, \omega}, p^{u, f, \epsilon}),$$

720 $\mathfrak{U} := \mathbf{U}$, $\mathfrak{V} := \{f \in K : \|f\|_V \leq 1\}$ and $\ell(\epsilon) = |B_\epsilon(\eta_0)|$. Since the minimisation
 721 problem in (7) is uniquely solvable and in view of Lemma 2.4 Assumptions (A0) and
 722 (A1) are satisfied. We turn to verifying (A2) and (A3) next.

723 Let (ϵ_n) be an arbitrary null-sequence and let (f_n) be a sequence in K converging
 724 weakly in V to $f \in K$. Thanks to Assumption 4.2 the sequence (\bar{u}_n) , $\bar{u}_n := \bar{u}^{f_n, \omega_{\epsilon_n}}$
 725 converges strongly in $L_1(0, T; C(\bar{B}_\delta(\eta_0)))$ to $\bar{u} = \bar{u}^{f, \omega} \in L_1(0, T; C(\bar{B}_\delta(\eta_0)))$. There-
 726 fore (recall the notation $\bar{p}^{f, \omega_{\epsilon_n}} = p^{\bar{u}_n, f, \omega_{\epsilon_n}}$) we obtain

$$727 \quad (139) \quad \begin{aligned} \frac{G(\epsilon_n, \bar{u}_n, f_n) - G(0, \bar{u}_n, f_n)}{|B_{\epsilon_n}(\eta_0)|} &= - \frac{1}{|B_{\epsilon_n}(\eta_0)|} \int_0^T \int_{B_{\epsilon_n}(\eta_0)} \bar{u}_n \bar{p}^{f_n, \epsilon_n} \, dx \, dt \\ &= - \frac{1}{|B_{\epsilon_n}(\eta_0)|} \int_0^T \int_{B_{\epsilon_n}(\eta_0)} \bar{u}_n (\bar{p}^{f_n, \epsilon_n} - \bar{p}^{f, \omega}) \, dx \, dt \\ &\quad - \frac{1}{|B_{\epsilon_n}(\eta_0)|} \int_0^T \int_{B_{\epsilon_n}(\eta_0)} (\bar{u}_n - \bar{u}) \bar{p}^{f, \omega} \, dx \, dt \\ &\quad - \frac{1}{|B_{\epsilon_n}(\eta_0)|} \int_0^T \int_{B_{\epsilon_n}(\eta_0)} \bar{u}(x, t) \bar{p}^{f, \omega}(x, t) \, dx \, dt. \end{aligned}$$

728 Further for all n ,

$$729 \quad (140) \quad \frac{1}{|B_{\epsilon_n}(\eta_0)|} \left| \int_0^T \int_{B_{\epsilon_n}(\eta_0)} (\bar{u}_n - \bar{u}) \bar{p}^{f_n, \omega} dx dt \right| \\ \leq \| \bar{p}^{f_n, \omega} \|_{C([0, T] \times \bar{B}_\delta(\eta_0))} \| \bar{u}_n - \bar{u} \|_{L_1(0, T; C(\bar{B}_\delta(\eta_0)))}$$

730 and

$$731 \quad (141) \quad \frac{1}{|B_{\epsilon_n}(\eta_0)|} \left| \int_0^T \int_{B_{\epsilon_n}(\eta_0)} \bar{u}_n (\bar{p}^{f_n, \epsilon_n} - \bar{p}^{f_n, \omega}) dx dt \right| \\ \leq \| \bar{u}_n \|_{L_1(0, T; C(\bar{B}_\delta(\eta_0)))} \| \bar{p}^{f_n, \epsilon_n} - \bar{p}^{f_n, \omega} \|_{C([0, T] \times \bar{B}_\delta(\eta_0))}.$$

732 Since $x \mapsto \int_0^T \bar{u}(x, t) \bar{p}^{f, \omega}(x, t) dt$ is continuous in a neighborhood of η_0 we also have

$$733 \quad (142) \quad \lim_{n \rightarrow \infty} \frac{1}{|B_{\epsilon_n}(\eta_0)|} \int_0^T \int_{B_{\epsilon_n}(\eta_0)} \bar{u}(x, t) \bar{p}^{f, \omega}(x, t) dx dt = \int_0^T \bar{u}(\eta_0, t) \bar{p}^{f, \omega}(\eta_0, t) dt.$$

734 Hence in view of (139) we obtain

$$735 \quad (143) \quad \lim_{n \rightarrow \infty} \frac{G(\epsilon_n, \bar{u}_n, f_n) - G(0, \bar{u}_n, f_n)}{|B_{\epsilon_n}(\eta_0)|} = - \int_0^T \bar{u}(\eta_0, t) \bar{p}^{f, \omega}(\eta_0, t) dt$$

736 Next let $\bar{u}_{n,0} := \bar{u}^{f_n, 0}$. Then we can show in a similar manner as (143) that

$$737 \quad (144) \quad \lim_{n \rightarrow \infty} \frac{G(\epsilon_n, \bar{u}_{n,0}, f_n) - G(0, \bar{u}_{n,0}, f_n)}{|B_{\epsilon_n}(\eta_0)|} = - \int_0^T \bar{u}(\eta_0, t) \bar{p}^{f, \omega}(\eta_0, t) dt$$

738 Hence choosing (f_n) to be a constant sequence we see that (A2) is satisfied.

739 But also (A3) is satisfied since according to Lemma 3.14 we find for every null-
740 sequence (τ_n) in $[0, \tau_X]$ and every sequence (f_n) , $f_n \in \mathfrak{X}_2(\omega_{\tau_n})$, a subsequence (f_{n_k})
741 and $f \in \mathfrak{X}_2(\omega)$, such that $f_{n_k} \rightharpoonup f$ in $H_0^1(\Omega)$ as $k \rightarrow \infty$. Now we use (143) and (144)
742 with f_n replaced by this choice of f_{n_k} , and conclude that (A3) holds.

743 **5. Numerical approximation of the optimal shape problem.** In this sec-
744 tion we discuss the formulation of numerical methods for optimal positioning and
745 design which are based on the formulae introduced in previous sections. We begin
746 by introducing the discretisation of the system dynamics and the associated linear-
747 quadratic optimal control problem. Then, the optimal actuator design problem is
748 addressed by approximating the shape and topological derivatives, which are embed-
749 ded into a gradient-based approach and a level-set method, respectively.

750 **5.1. Discretisation and Riccati equation.** Let $T > 0$. We choose the spaces
751 $K = H_0^1(\Omega)$ and $\mathcal{U} = \mathbf{R}$, so that the control space \mathbf{U} is equal to $L_2(0, T; \mathbf{R})$. The cost
752 functional reads

$$753 \quad (145) \quad \mathcal{J}_1(\omega, f) = \inf_{u \in \mathbf{U}} J(\omega, u, f) = \int_0^T \|y(t)\|_{L^2(\Omega)}^2 + \gamma |u(t)|^2 dt + \alpha (|\omega| - c)^2, \quad \alpha > 0,$$

754

755 where y is the solution of the state equation

$$756 \quad (146) \quad \partial_t y(x, t) = \sigma \Delta y(x, t) + \chi_\omega(x) u(t) \quad (x, t) \in \Omega \times (0, T],$$

$$757 \quad (147) \quad y(x, t) = 0 \quad (x, t) \in \partial\Omega \times (0, T],$$

$$758 \quad (148) \quad y(0, x) = f \quad x \in \Omega,$$

760 and Ω is a polygonal domain. The cost J in (145) includes the additional term
 761 $\alpha(|\omega| - c)^2$ which accounts for the volume constraint $|\omega| = c$ in a penalty fashion. This
 762 slightly modifies the topological derivative formula, as it will be shown later. We derive
 763 a discretised version of the dynamics (146)-(148) via the method of lines. For this, we
 764 introduce a family of finite-dimensional approximating subspaces $V_h \subset H_0^1(\Omega)$, where
 765 h stands for a discretisation parameter typically corresponding to gridsize in finite
 766 elements/differences, but which can also be related to a spectral approximation of the
 767 dynamics. For each $f_h \in V_h$, we consider a finite-dimensional nodal/modal expansion
 768 of the form

$$769 \quad (149) \quad f_h = \sum_{j=1}^N f_j \phi_j, \quad f_j \in \mathbf{R}, \phi_j \in V_h,$$

where $\{\phi_i\}_{i=1}^N$ is a basis of V_h . We denote the vector of coefficients associated to
 the expansion by $\underline{f}_h := (f_1, \dots, f_N)^\top$. In the method of lines, we approximate the
 solution y of (146)-(148) by a function y_h in $C^1([0, T]; V_h(\Omega))$ of the type

$$y_h(x, t) = \sum_{j=1}^N y_j(t) \phi_j(x),$$

770 for which we follow a standard Galerkin ansatz. Inserting y_h in the weak formulation
 771 (2) and testing with $\varphi = \phi_k$, $k = 1, \dots, N$ leads to the following system of ordinary
 772 equations,

$$773 \quad (150) \quad \dot{\underline{y}}_h(t) = A_h \underline{y}_h(t) + B_h u_h(t) \quad t \in (0, T], \quad \underline{y}_h(0) = \underline{f}_h,$$

774 where $M_h, K_h \in \mathbf{R}^{N \times N}$ and $B_h, \underline{f}_h \in \mathbf{R}^N$ are given by

$$775 \quad (151) \quad A_h = -M_h^{-1} S_h, \quad B_h = M_h^{-1} \hat{B}_h, \quad \underline{f}_h := M_h^{-1} \hat{\underline{f}}_h,$$

776 with

$$777 \quad (152) \quad (M_h)_{ij} = (\phi_i, \phi_j)_{L_2}, \quad (S_h)_{ij} = \sigma(\nabla \phi_i, \nabla \phi_j)_{L_2}, \\ (\hat{B}_h)_j = (\chi_\omega, \phi_j)_{L_2}, \quad (\hat{\underline{f}}_h)_j := (f, \phi_j)_{L_2}, \quad i, j = 1, \dots, N.$$

778 Note that $\underline{y}_h = \underline{y}_h^{u_h, \underline{f}_h, \omega}$ depends on f_h , u_h , and ω . Given a discrete initial condition
 779 $f_h \in V_h(\Omega)$, the discrete costs are defined by
 (153)

$$780 \quad \mathcal{J}_{1,h}(\omega, f_h) := \inf_{u_h \in \mathbf{U}} J_h(\omega, u, f_h) = \inf_{u_h \in \mathbf{U}} \int_0^T (\underline{y}_h)^\top M_h \underline{y}_h + \gamma |u_h(t)|^2 dt + \alpha(|\omega| - c)^2,$$

781 and

$$782 \quad (154) \quad \mathcal{J}_{2,h}(\omega) = \sup_{\substack{f_h \in V_h \\ \|f_h\|_{H^1} \leq 1}} \mathcal{J}_{1,h}(\omega, f_h).$$

783 The solution of the linear-quadratic optimal control problem in (153) is given by

$$784 \quad \bar{u}^{\omega, f_h}(t) = -\gamma^{-1} B_h^\top \Pi_h(t) \underline{y}_h,$$

785 where $\Pi_h \in R^{N \times N}$ satisfies the differential matrix Riccati equation

$$786 \quad -\frac{d}{dt}\Pi_h = A_h\Pi_h + \Pi_h A_h - \Pi_h B_h \gamma^{-1} B_h^\top \Pi_h + M_h \quad \text{in } [0, T], \quad \Pi_h(T) = 0.$$

787 The coefficient vector of the discrete adjoint state $\bar{p}_h^{f_h, \omega}(t)$ at time t can be recovered
788 directly by $\bar{p}_h^{f_h, \omega}(t) = 2\Pi_h(t)\underline{y}_h(t)$. Let us define the discrete analog of (38),

$$789 \quad (155) \quad \mathfrak{X}_{2,h}(\omega) := \{\bar{f}_h \in V_h : \sup_{\substack{f_h \in V_h \\ \|f_h\|_{H^1} \leq 1}} \mathcal{J}_{1,h}(\omega, f_h) = \mathcal{J}_{1,h}(\omega, \bar{f}_h)\}.$$

790 Since we have the relation

$$791 \quad (156) \quad \mathcal{J}_{1,h}(\omega, f_h) = (\Pi_h(0)\underline{f}_h, \underline{f}_h)_{L_2} + \alpha(|\omega| - c)^2,$$

792 the maximisers $f_h \in \mathfrak{X}_{2,h}(\omega)$ can be computed by solving the generalised Eigenvalue
793 problem: find $(\lambda_h, f_h) \in \mathbf{R} \times V_h$ such that

$$794 \quad (157) \quad (\Pi_h(0) - \lambda_h S_h)\underline{f}_h = 0.$$

795 The biggest $\lambda_h = \lambda_h^{max}$ is then precisely the value $\mathcal{J}_{2,h}(\omega)$ and the normalised Eigen-
796 vectors for this Eigenvalue are the elements in $\mathfrak{X}_{2,h}(\omega)$:

$$797 \quad (158) \quad \mathfrak{X}_{2,h}(\omega) = \{f_h : \underline{f}_h \in \ker((\Pi_h(0) - \lambda_h^{max} K_h)) \text{ and } \|\underline{f}_h\| = 1\}.$$

798 **REMARK 5.1.** *It is readily checked that if $f_h \in \mathfrak{X}_{2,h}(\omega)$, then also $-f_h \in \mathfrak{X}_{2,h}(\omega)$.
799 So if the Eigenspace for the largest eigenvalue is one-dimensional we have $\mathfrak{X}_{2,h}(\omega) =$
800 $\{f_h, -f_h\}$. However, we know according to Corollary 3.8 (now in a discrete setting)
801 that*

$$802 \quad (159) \quad \mathcal{T}\mathcal{J}_{1,h}(\omega, f_h)(\eta_0) = \mathcal{T}\mathcal{J}_{1,h}(\omega, -f_h)(\eta_0)$$

803 for all $\eta_0 \in \Omega \setminus \partial\omega$ and $f_h \in V_h$. Hence we can evaluate the topological derivative
804 $\mathcal{T}\mathcal{J}_{2,h}(\omega)$ by picking either f_h or $-f_h$. A similar argumentation holds for the shape
805 derivative.

806 **5.2. Optimal actuator positioning: Shape derivative.** Here we precise the
807 gradient algorithm based upon a numerical realisation of the shape derivative. We
808 consider (146)-(148) with its discretisation (150). Given a simply connected actuator
809 $\omega_0 \subset \Omega$ we employ the shape derivative of \mathcal{J}_1 to find the optimal position. Let $f_h \in V_h$.
810 According to Corollary 3.6 the derivative of $\mathcal{J}_{1,h}$ in the case $\mathcal{U} = \mathbf{R}$ is given by

$$811 \quad (160) \quad D\mathcal{J}_{1,h}(\omega, f_h)(X) = - \int_{\partial\omega} \bar{u}_h^{f_h, \omega}(t) \int_0^T \bar{p}_h^{f_h, \omega}(s, t)(X(s) \cdot \nu(s)) ds dt$$

812 for $X \in \mathring{C}^1(\bar{\Omega}, \mathbf{R}^d)$. We assume that $\omega \Subset \Omega$. We define the vector $b \in \mathbf{R}^d$ with the
813 components

$$814 \quad (161) \quad b_i := \int_{\partial\omega} \bar{u}_h^{f_h, \omega}(t) \int_0^T \bar{p}_h^{f_h, \omega}(s, t)(e_i \cdot \nu(s)) ds dt,$$

815 where e_i denotes the canonical basis of \mathbf{R}^d . From this we can construct an admissible
816 descent direction by choosing any $\tilde{X} \in \mathring{C}^1(\bar{\Omega}, \mathbf{R}^d)$ with $\tilde{X}|_{\partial\omega} = b$. Then it is obvious

817 that $D\mathcal{J}_{1,h}(\omega, f_h)(\tilde{X}) \leq 0$. Let us use the notation $b = -\nabla\mathcal{J}_{1,h}(\omega, f_h)$. We write
 818 $(\text{id} + t\nabla\mathcal{J}_{1,h}(\omega, f_h))(\omega)$ to denote the moved actuator ω via the vector b . Note that
 819 only the position, but not the shape of ω changes by this operation. We refer to this
 820 procedure as Algorithm 1 below.

Algorithm 1 Shape derivative-based gradient algorithm for actuator positioning

Input: $\omega_0 \in \mathfrak{D}(\Omega)$, $f_h \in V_h$, $b_0 := -\nabla\mathcal{J}_{1,h}(\omega_0, f_h)$, $n = 0$, $\beta_0 > 0$, and $\epsilon > 0$.
while $|b_n| \geq \epsilon$ **do**
 if $\mathcal{J}_{1,h}((\text{id} + \beta_n b_n)(\omega_n), f_h) < \mathcal{J}_{1,h}(\omega_n, f_h)$ **then**
 $\beta_{n+1} \leftarrow \beta_n$
 $\omega_{n+1} \leftarrow (\text{id} + \beta_n b_n)(\omega_n)$
 $b_{n+1} \leftarrow -\nabla\mathcal{J}_{1,h}(\omega_{n+1}, f_h)$
 $n \leftarrow n + 1$
 else
 decrease β_n
 end if
end while
return optimal actuator positioning ω_{opt}

821 **5.3. Optimal actuator design: Topological derivative.** As for the shape
 822 derivative, we now introduce a numerical approximation of the topological deriva-
 823 tive formula which is embedded into a level-set method to generate an algorithm
 824 for optimal actuator design, i.e. including both shaping and position. According to
 825 Theorem 4.4 the discrete topological derivative of $\mathcal{J}_{1,h}$ is given by
 (162)

$$826 \quad \mathcal{T}\mathcal{J}_{1,h}(\omega, f_h)(\eta_0) = \begin{cases} \int_0^T \bar{u}_h^{f_h, \omega}(t) \bar{p}_h^{f_h, \omega}(\eta_0, t) dt - 2\alpha(|\omega| - c) & \text{if } \eta_0 \in \omega, \\ - \int_0^T \bar{u}_h^{f_h, \omega}(t) \bar{p}_h^{f_h, \omega}(\eta_0, t) dt + 2\alpha(|\omega| - c) & \text{if } \eta_0 \in \Omega \setminus \bar{\omega}, \end{cases}$$

827 The level-set method is well-established in the context of shape optimisation and
 828 shape derivatives [2]. Here we use a level-set method for topological sensitivities as
 829 proposed in [4]. We recall that compared to the the formulation based on shape sensi-
 830 tivities, the topological approach has the advantage that multi-component actuators
 831 can be obtained via splitting and merging.

832 For a given actuator $\omega \subset \Omega$, we begin by defining the function

$$833 \quad g_h^{f_h, \omega}(\zeta) = - \int_0^T \bar{u}_h^{f_h, \omega}(t) \bar{p}_h^{f_h, \omega}(\zeta, t) dt + 2\alpha(|\omega| - c), \quad \zeta \in \bar{\Omega}$$

834 which is continuous since the adjoint is continuous in space. Note that $\bar{p}_h^{f_h, \omega}$ and
 835 $\bar{u}_h^{f_h, \omega}$ depend on the actuator ω . For other types of state equations where the shape
 836 variable enters into the differential operator (e.g. transmission problems [3]) this may
 837 not be the case and thus it particular of our setting. The necessary optimality condi-
 838 tion for the cost function $\mathcal{J}_{1,h}(\omega, f_h)$ using the topological derivative are formulated
 839 as

$$840 \quad (163) \quad \begin{aligned} g_h^{f_h, \omega}(x) &\leq 0 && \text{for all } x \in \omega, \\ g_h^{f_h, \omega}(x) &\geq 0 && \text{for all } x \in \Omega \setminus \bar{\omega}. \end{aligned}$$

841 Since $g_h^{f_h, \omega}$ is continuous this means that $g_h^{f_h, \omega}$ vanishes on $\partial\omega$ and hence

$$842 \quad (164) \quad \int_0^T \bar{u}_h^{f_h, \omega}(t) \bar{p}_h^{f_h, \omega}(\zeta, t) dt = 2\alpha(|\omega| - c), \quad \text{for all } \zeta \in \partial\omega.$$

843 An (actuator) shape ω that satisfies (163) is referred to as stationary (actuator) shape.
844 It follows from (162) and (163), that $g_h^{f_h, \omega}$ vanishes on the actuator boundary $\partial\omega$ of
845 a stationary shape ω .

846 We now describe the actuator ω via an arbitrary level-set function $\psi_h \in V_h$, such
847 that $\omega = \{x \in \Omega : \psi_h(x) < 0\}$ is achieved via an update of an initial guess ψ_h^0

$$848 \quad (165) \quad \psi_h^{n+1} = (1 - \beta_n)\psi_h^n + \beta_n \frac{g_h^{f_h, \omega_n}}{\|g_h^{f_h, \omega_n}\|}, \quad \omega_n := \{x \in \Omega : \psi_h^n(x) < 0\},$$

849 where β_n is the step size of the method. The idea behind this update scheme is the
850 following: if $\psi_h^n(x) < 0$ and $g_h^{f_h, \omega_n}(x) > 0$, then we add a positive value to the level-
851 set function, which means that we aim at removing actuator material. Similarly, if
852 $\psi_h^n(x) > 0$ and $g_h^{f_h, \omega_n}(x) < 0$, then we create actuator material. In all the other cases
853 the sign of the level-sets remains unchanged. We present our version of the level-set
854 algorithm in [4], which we refer to as Algorithm 2.

Algorithm 2 Level set algorithm for optimal actuator design

Input: $\psi_h^0 \in V_h(\Omega)$, $\omega_0 := \{x \in \bar{\Omega}, \psi_h^0(x) < 0\}$, $\beta_0 > 0$, $f_h \in V_h$, and $\epsilon > 0$.

while $\|\omega_{n+1} - \omega_n\| \geq \epsilon$ **do**

if $\mathcal{J}_{1,h}(\{\psi_h^{n+1} < 0\}, f_h) < \mathcal{J}_{1,h}(\{\psi_h^n < 0\}, f_h)$ **then**

$$\psi_h^{n+1} \leftarrow (1 - \beta_n)\psi_h^n + \beta_n \frac{g_h^{f_h, \omega_n}}{\|g_h^{f_h, \omega_n}\|}$$

$$\beta_{n+1} \leftarrow \beta_n$$

$$\omega_{n+1} \leftarrow \{\psi_h^{n+1} < 0\}$$

$$n \leftarrow n + 1$$

else

 decrease β_n

end if

end while

return optimal actuator ω_{opt}

855 Algorithm 2 is embedded inside a continuation approach over the quadratic
856 penalty parameter α in (153), leading to actuators which approximate the size con-
857 straint in a sensible way, as opposed to a single solve with a large value of α .

858 Finally, for the functional $\mathcal{J}_2(\omega)$ we may employ similar algorithms for shape and
859 topological derivatives. We update the initial condition $f_h \in \mathfrak{X}_{2,h}(\omega)$ at each iteration
860 whenever the actuator ω is modified.

861 **6. Numerical tests.** We present a series of one and two-dimensional numerical
862 tests exploring the different capabilities of the developed approach.

863 *Test parameters and setup.* We establish some common settings for the experi-
864 ments. For the 1D tests, we consider a piecewise linear finite element discretisation
865 with 200 elements over $\Omega = (0, 1)$, with $\gamma = 10^{-3}$, $\sigma = 0.01$, $c = 0.2$, and $\epsilon = 10^{-7}$.
866 For the 2D tests, we resort to a Galerkin ansatz where the basis set is composed by the
867 eigenfunctions of the Laplacian with Dirichlet boundary conditions over $\Omega = (0, 1)^2$.

868 We utilize the first 100 eigenfunctions. This idea has been previously considered in the
 869 context of optimal actuator positioning in [18], and its advantage resides in the lower
 870 computational burden associated to the Riccati solve. The actuator size constraint is
 871 set to $c = 0.04$. An important implementation aspect relates to the numerical approx-
 872 imation of the linear-quadratic optimal control problem for a given actuator. For the
 873 sake of simplicity, we consider the infinite horizon version of the costs \mathcal{J}_1 and \mathcal{J}_2 . In
 874 this way, the optimal control problems are solved via an Algebraic Riccati Equation
 875 approach. The additional calculations associated to \mathcal{J}_2 and the set $\mathfrak{X}_2(\omega)$ are reduced
 876 to a generalized eigenvalue problem involving the Riccati operator Π_h . The shape
 877 and topological derivative formulae involving the finite horizon integral of u and p are
 878 approximated with a sufficiently large time horizon, in this case $T = 1000$.

Actuator size constraint. While in the abstract setting the actuator size constraint determines the admissible set of configurations, its numerical realisation follows a penalty approach, i.e. $\mathcal{J}_1(\omega, f)$ is as in (145),

$$\mathcal{J}_1(\omega, f) = \mathcal{J}_1^{LQ}(\omega, f) + \mathcal{J}_1^\alpha(\omega),$$

879 where $\mathcal{J}_1^{LQ}(\omega, f)$ is the original linear-quadratic (LQ) performance measure, and
 880 $\mathcal{J}_1^\alpha(\omega) = \alpha(|\omega| - c)^2$ is a quadratic penalization from the reference size. The cost
 881 \mathcal{J}_2 is treated analogously. In order to enforce the size constraint as much as possible
 882 and to avoid suboptimal configurations, the quadratic penalty is embedded within a
 883 homotopy/continuation loop. For a low initial value of α , we perform a full solve of
 884 Algorithm 2, which is then used to initialize a subsequent solve with an increased
 885 value of α . As it will be discussed in the numerical tests, for sufficiently large val-
 886 ues of α and under a gradual increase of the penalty, results are accurate within the
 887 discretisation order.

888 *Algorithm 2 and level-set method.* The main aspect of Algorithm 2 is the level-
 889 set update of the function ψ_h^{n+1} which dictates the new actuator shape. In order to
 890 avoid the algorithm to stop around suboptimal solutions, we proceed to reinitialize the
 891 level-set function every 50 iterations. This is a well-documented practice for the level-
 892 set method, and in particular in the context of shape/topology optimisation [2, 4].
 893 Our reinitialization consists of reinitialising ψ_h^{n+1} to be the signed distance function
 894 of the current actuator. The signed distance function is efficiently computed via the
 895 associated Eikonal equation, for which we implement the accelerated semi-Lagrangian
 896 method proposed in [1], with an overall CPU time which is negligible with respect to
 897 the rest of the algorithm.

898 *Practical aspects.* All the numerical tests have been performed on an Intel Core i7-
 899 7500U with 8GB RAM, and implemented in MATLAB. The solution of the LQ control
 900 problem is obtained via the ARE command, the optimal trajectories are integrated
 901 with a fourth-order Runge-Kutta method in time. While a single LQ solve does not
 902 take more than a few seconds in the 2D case, the level-set method embedded in a
 903 continuation loop can scale up to approximately 30 mins. for a full 2D optimal shape
 904 solve.

905 **6.1. Optimal actuator positioning through shape derivatives.** In the first
 906 two tests we study the optimal positioning problem (11) of a single-component ac-
 907 tuator of fixed width 0.2 via the gradient-based approach presented in Algorithm 1.
 908 Tests are carried out for a given initial condition $y_0(x)$, i.e. the \mathcal{J}_1 setting.

909 *Test 1.* We start by considering $y_0(x) = \sin(\pi x)$, so the test is fully symmetric,
 910 and we expect the optimal position to be centered in the middle of the domain, i.e.
 911 at $x = 0.5$. Results are illustrated in Figure 1, where it can be observed that as

912 the actuator moves from its initial position towards the center, the cost \mathcal{J}_1 decays
 913 until reaching a stationary value. Results are consistent with the result obtained by
 914 inspection (Figure 1 left), where the location of the center of the actuator has been
 moved throughout the entire domain.

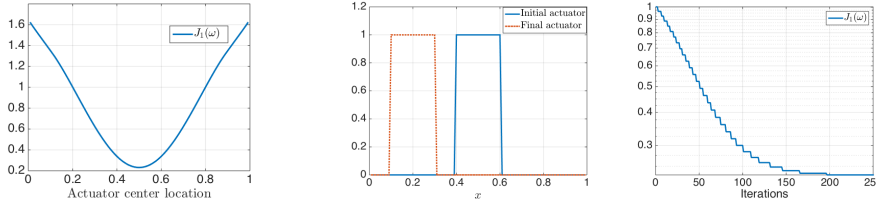


FIG. 1. *Test 1. Left: different single-component actuators with different centers have been spanned over the domain, locating the minimum value of \mathcal{J}_1 for the center at $x = 0.5$. Center: starting from an initial guess for the actuator far from 0.5, the gradient-based approach of Algorithm 1 locates the optimal position in the middle. Right: as the actuator moves towards the center in the subsequent iterations of Algorithm 1, the value \mathcal{J}_1 decays until reaching a stationary point.*

915

916

917 *Test 2.* We consider the same setting as in the previous test, but we change
 918 the initial condition of the dynamics to be $y_0(x) = 100|x - 0.7|^4 + x(x - 1)$, so the
 919 setting is asymmetric and the optimal position is different from the center. Results
 are shown in Figure 2, where the numerical solution coincides with the result obtained
 by inspecting all the possible locations.

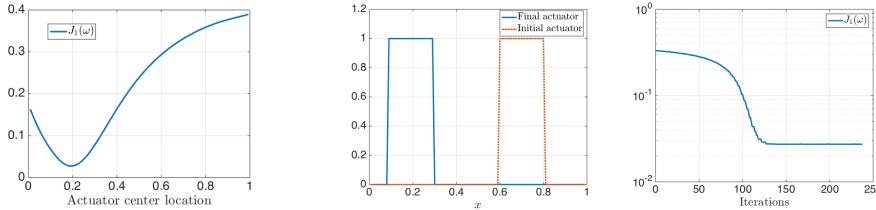


FIG. 2. *Test 2. Left: inspecting different values of \mathcal{J}_1 by spanning actuators with different centers, the optimal center location is found to be close to 0.2. Center: the gradient-based approach steers the initial actuator to the optimal position. Right: the value \mathcal{J}_1 decays until reaching a stationary point, which coincides with the minimum for the first plot on the left.*

920

921

922

923

924

925

926

927

928

929

930

931

932

933

934

6.2. Optimal actuator design through topological derivatives. In the following series of experiments we focus on 1D optimal actuator design, i.e. problems (9) and (10) without any further parametrisation of the actuator, thus allowing multi-component structures. For this, we consider the approach combining the topological derivative, with a level-set method, as summarized in Algorithm 2.

Test 3. For $y_0(x) = \max(\sin(3\pi x), 0)^2$, results are presented in Figures 3 and 4. As it can be expected from the symmetry of the problem, and from the initial condition, the actuator splits into two equally sized components. We carried out two types of tests, one without and one with a continuation strategy with respect to α . Without a continuation strategy, choosing $\alpha = 10^3$ we obtain the result depicted in Figure 3 (b). With a continuation strategy, as the penalty increases, the size of the components decreases until approaching the total size constraint. The behavior of this continuation approach is shown in Table 1. When α is increased, the size of the actuator tends to 0.2, the reference size, while the LQ part of \mathcal{J}_1 , tends to a

935 stationary value. For a final value of $\alpha = 10^4$, the overall cost \mathcal{J}_1 obtained via the
 936 continuation approach is approx. 80 times smaller than the value obtained without
 937 any initialisation procedure, see Figure 3 (b)-(d). Figure 4 illustrates some basic
 938 relevant aspects of the level-set approach, such as the update of the shape (left), the
 939 computation of the level-set update upon β_n and ψ_h^n (middle), and the decay of the
 940 value J_1 (right).

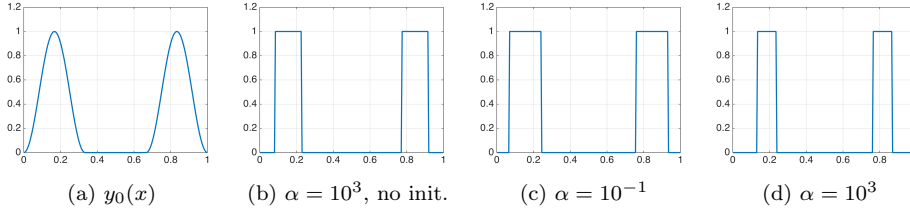


FIG. 3. *Test 3.* (a) Initial condition $y_0(x) = \max(\sin(3\pi x), 0)^2$. (b) Optimal actuator for $\alpha = 10^3$, without initialization via increasing penalization. (c) Optimal actuator for $\alpha = 10^{-1}$, subsequently used in the quadratic penalty approach. (d) Optimal actuator for $\alpha = 10^3$, via increasing penalization.

α	\mathcal{J}_1	\mathcal{J}_1^{LQ}	\mathcal{J}_1^α (size)	iterations
0.1	1.84×10^{-2}	1.62×10^{-2}	2.30×10^{-3} (0.35)	225
1	2.35×10^{-2}	2.26×10^{-2}	9.10×10^{-4} (0.23)	226
10	2.56×10^{-2}	2.46×10^{-2}	1.00×10^{-3} (0.21)	316
10^2	3.46×10^{-2}	2.46×10^{-2}	1.00×10^{-2} (0.21)	226
10^3	0.12	2.46×10^{-2}	1.00×10^{-1} (0.21)	226
10^{3*}	8.18	8.00×10^{-2}	8.10 (0.29)	629

TABLE 1

Test 3. optimisation values for $y_0(x) = \max(\sin(3\pi x), 0)^2$. Each row is initialized with the optimal actuator corresponding to the previous one, except for the last row with $\alpha = 10^{3*}$, illustrating that incorrectly initialized solves lead to suboptimal solutions. The reference size for the actuator is 0.2 .

941 *Test 4.* We repeat the setting of Test 3 with a nonsymmetric initial condition
 942 $y_0(x) = \sin(3\pi x)^2 \chi_{\{x < 2/3\}}(x)$. Results are presented in Table 2 and Figure 5, which
 943 illustrate the effectivity of the continuation approach, which generates an optimal
 944 actuator with two components of different size, see Figure 5d and compare with Figure
 945 5b.

946 *Test 5.* We now turn our attention to the optimal actuator design for the worst-
 947 case scenario among all the initial conditions, i.e. the \mathcal{J}_2 setting. Results are presented
 948 in Figure 6 and Table 3. The worst-case scenario corresponds to the first eigenmode
 949 of the Riccati operator (Figure 6a), which generates a two-component symmetric
 950 actuator (Figure 6d). This is only observed within the continuation approach. For a
 951 large value of α without initialisation, we obtain a suboptimal solution with a single
 952 component (last row of Table 3, Figure 6b).

953 *Test 6.* As an extension of the capabilities of the proposed approach, we explore
 954 the \mathcal{J}_2 setting with space-dependent diffusion. For this test, the diffusion operator

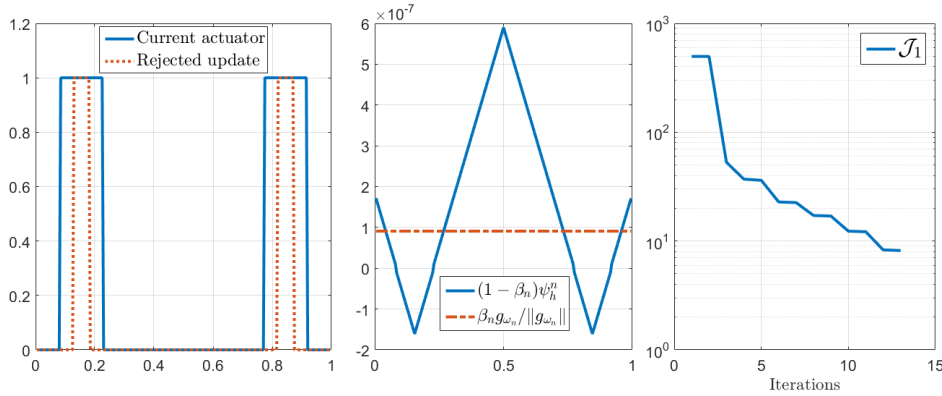


FIG. 4. Test 3. Level set method implemented in Algorithm 2. Left: starting from an initial actuator, the topological derivative of the cost is computed and an updated actuator is obtained. The new shape is evaluated according to its closed-loop performance. If the update is rejected, the parameter β_n is reduced. Middle: the level-set approach generates an update of the actuator shape based on the information from ψ_h^n , β_n and g_{ω_n} . Right: This iterative loop generates a decay in the total cost J_1 , (which accounts for both the closed-loop performance of the actuator and its volume constraint).

α	\mathcal{J}_1	\mathcal{J}_1^{LQ}	\mathcal{J}_1^α (size)	iterations
0.1	6.48×10^{-2}	6.31×10^{-2}	1.7×10^{-3} (0.33)	229
1	8.0×10^{-2}	6.31×10^{-2}	1.69-2 (0.33)	226
10	0.176	0.164	1.23×10^{-2} (0.235)	226
10^2	0.207	0.184	2.25×10^{-2} (0.215)	316
10^3	0.234	0.209	2.50×10^{-2} (0.195)	316
10^4	0.459	0.209	0.250 (0.195)	316
10^{4*}	9.09	9.66×10^{-2}	9 (0.23)	629

TABLE 2

Test 4. optimisation values for $y_0(x) = \sin(3\pi x)^2 \chi_{x < 2/3}(x)$. Each row is initialized with the optimal actuator corresponding to the previous one, except for the last row with $\alpha = 10^{4*}$, illustrating that incorrectly initialized solves lead to suboptimal solutions. The reference size for the actuator is 0.2 .

955 $\sigma \Delta y$ is rewritten as $\text{div}(\sigma(x) \nabla y)$, with $\sigma(x) = (1 - \max(\sin(9\pi x), 0)) \chi_{\{x < 0.5\}}(x) +$
 956 10^{-3} . Iterates of the continuation approach are presented in Table 4. Again, the
 957 lack of a proper initialization of Algorithm 2 with a large value of α leads to a poor
 958 satisfaction of both the size constraint and the LQ performance, which is solved via
 959 the increasing penalty approach. A two-component actuator present in the area of
 960 smaller diffusion is observed in Figure 7d.

961 **6.3. Two-dimensional optimal actuator design.** We now turn our attention
 962 into assessing the performance of Algorithm 2 for two-dimensional actuator topology
 963 optimisation. While this problem is computationally demanding, the increase of de-
 964 grees of freedom can be efficiently handled via modal expansions, as explained at the
 965 beginning of this Section. We explore both the \mathcal{J}_1 and \mathcal{J}_2 settings.

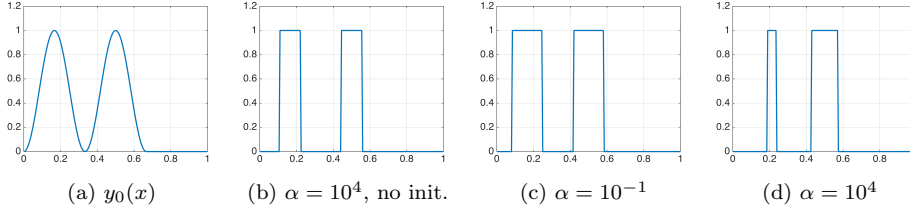


FIG. 5. *Test 4.* (a) Initial condition $y_0(x) = \sin(3\pi x)^2 \chi_{\{x < 2/3\}}(x)$. (b) Optimal actuator for $\alpha = 10^4$, without initialization via increasing penalization. (c) Optimal actuator for $\alpha = 10^{-1}$, subsequently used in the quadratic penalty approach. (d) Optimal actuator for $\alpha = 10^4$, via increasing penalization.

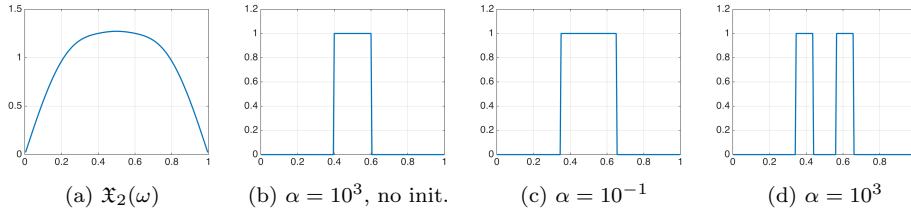


FIG. 6. *Test 5.* (a) First eigenmode of the Riccati operator, which corresponds to the set $\mathfrak{X}_2(\omega)$. (b) Optimal actuator for $\alpha = 10^3$, without initialization via increasing penalization. (c) Optimal actuator for $\alpha = 10^{-1}$, subsequently used in the quadratic penalty approach. (d) Optimal actuator for $\alpha = 10^3$, via increasing penalization.

α	\mathcal{J}_2	\mathcal{J}_2^{LQ}	$\mathcal{J}_2^\alpha(\text{size})$	iterations
0.1	0.402	0.401	1.1×10^{-3} (0.305)	307
1	0.369	0.364	4.0×10^{-4} (0.22)	225
10	0.343	0.342	1.0×10^{-3} (0.19)	228
10^2	0.352	0.342	1.0×10^{-2} (0.19)	226
10^3	0.442	0.342	0.1 (0.19)	226
10^{3*}	0.761	0.536	0.225 (0.215)	941

TABLE 3

Test 5. optimisation values for \mathcal{J}_2 . Each row is initialized with the optimal actuator corresponding to the previous one, except for the last row with $\alpha = 10^{3*}$. The reference size for the actuator is 0.2 .

966 *Test 7.* This experiment is a direct extension of Test 3. We consider a unilaterally
 967 symmetric initial condition $y_0(x_1, x_2) = \max(\sin(4\pi(x_1 - 1/8)), 0)^3 \sin(\pi x_2)^3$, induc-
 968 ing a two-component actuator. The desired actuator size is $c = 0.04$. The evolution
 969 of the actuator design for increasing values of the penalty parameter α is depicted in
 970 Figure 8. We also study the closed-loop performance of the optimal shape. For this
 971 purpose the running cost associated to the optimal actuator is compared against an
 972 ad-hoc design, which consists of a cylindrical actuator of desired size placed in the
 973 center of the domain, see Figure 9 . The closed-loop dynamics of the optimal actuator
 974 generate a stronger exponential decay compared to the uncontrolled dynamics and the

α	\mathcal{J}_2	\mathcal{J}_2^{LQ}	$\mathcal{J}_2^\alpha(\text{size})$	iterations
0.1	1.792	1.743	4.97×10^{-2} (0.908)	194
1	2.240	1.743	0.497 (0.908)	228
10	4.734	4.462	0.272 (0.365)	225
10^2	3.134	3.071	6.25×10^{-2} (0.175)	538
10^3	1.023	0.998	0.025 (0.195)	226
10^4	1.248	0.998	0.250 (0.195)	226
10^{4*}	28.19	3.195	25.0 (0.25)	673

TABLE 4

Test 6. \mathcal{J}_2 values with space-dependent diffusion $\sigma(x) = (1 - \max(\sin(9\pi x), 0))\chi_{\{x < 0.5\}}(x) + 10^{-3}$. Each row is initialized with the optimal actuator corresponding to the previous one, except for the last row with $\alpha = 10^{4*}$. The reference size for the actuator is 0.2.

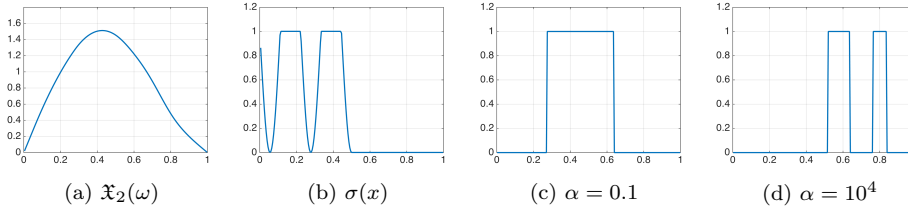


FIG. 7. Test 6. (a) First eigenmode of the Riccati operator, which corresponds to the set $\mathfrak{X}_2(\omega)$. (b) space-dependent diffusion coefficient $\sigma(x) = (1 - \max(\sin(9\pi x), 0))\chi_{\{x < 0.5\}}(x) + 10^{-3}$. (c) Optimal actuator for $\alpha = 10$, subsequently used in the quadratic penalty approach. (d) Optimal actuator for $\alpha = 10^4$, via increasing penalization.

975 ad-hoc shape.

976 *Test 8.* In an analogous way as in Test 5, we study the optimal design problem
 977 associated to \mathcal{J}_2 . The first eigenmode of the Riccati operator is shown in Figure 10a.
 978 The increasing penalty approach (Figs. 10c to 10f) shows a complex structure, with
 979 a hollow cylinder and four external components. The performance of the closed-loop
 980 optimal solution is analysed in Figure 11, with a considerably faster decay compared
 981 to the uncontrolled solution, and to the ad-hoc design utilised in the previous test.

982 **Concluding remarks.** In this work we have developed an analytical and compu-
 983 tational framework for optimisation-based actuator design. We derived shape and
 984 topological sensitivities formulas which account for the closed-loop performance of a
 985 linear-quadratic controller associated to the actuator configuration. We embedded
 986 the sensitivities into gradient-based and level-set methods to numerically realise the
 987 optimal actuators. Our findings seem to indicate that from a practical point of view,
 988 shape sensitivities are a good alternative whenever a certain parametrisation of the
 989 actuator is fixed in advance and only optimal position is sought. Topological sensi-
 990 tivities are instead suitable for optimal actuator design in a wider sense, allowing the
 991 emergence of nontrivial multi-component structures, which would be difficult to guess
 992 or parametrise a priori. This is a relevant fact, as most of the engineering literature
 993 associated to computational optimal actuator positioning is based on heuristic meth-
 994 ods which strongly rely on experts' knowledge and tuning. Extensions concerning

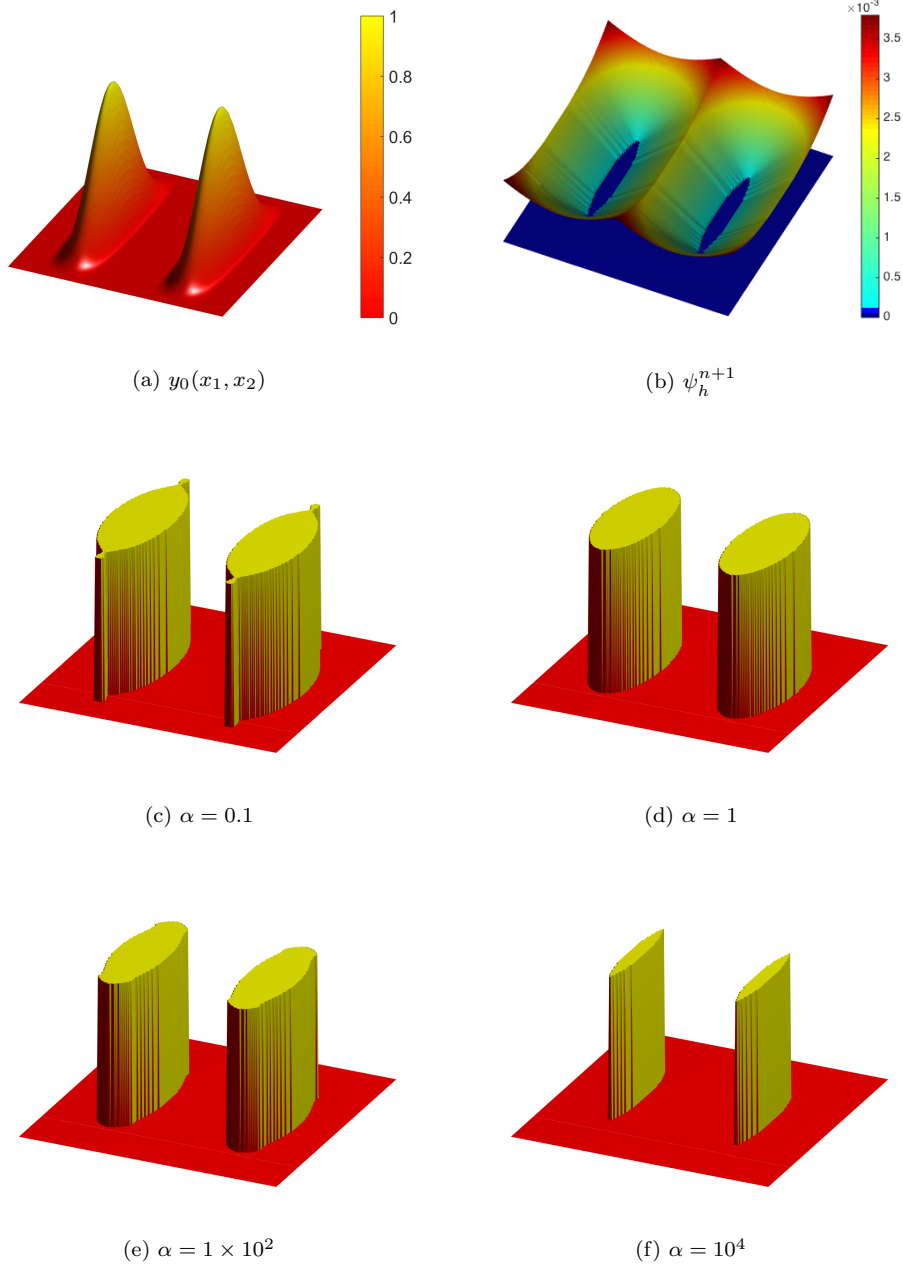


FIG. 8. Test 7. (a) initial condition $y_0(x_1, x_2) = \max(\sin(4\pi(x_1 - 1/8)), 0)^3 \sin(\pi x_2)^3$ for \mathcal{J}_1 optimisation. (b) within the level-set method, the actuator is updated according to the zero level-set of the function ψ_h^{n+1} . (c) to (f) optimal actuators for different volume penalties.

995 robust control design and semilinear parabolic equation are in our research roadmap.

996 **Appendix.**

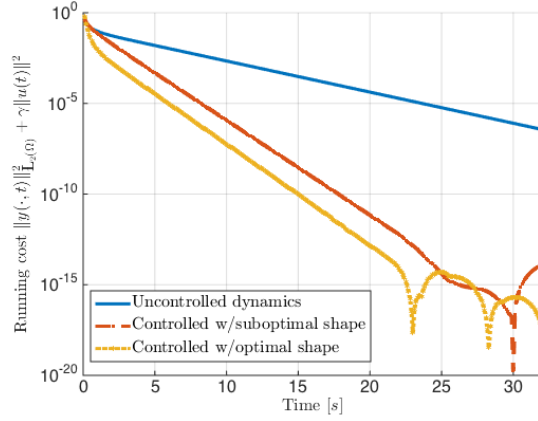


FIG. 9. Test 7. Closed-loop performance for different shapes. The running cost in \mathcal{J}_1 is evaluated for uncontrolled dynamics ($u \equiv 0$), an ad-ho cylindrical actuator located in the center of the domain, and the optimal shape (Figure 8f). Closed-loop dynamics of the optimal shape decay faster.

997 **Differentiability of maximum functions.** In order to prove Lemma 3.17 we
 998 recall the following Danskin-type lemmas.

999 Let \mathfrak{V}_1 be a nonempty set and let $\mathcal{G} : [0, \tau] \times \mathfrak{V}_1 \rightarrow \mathbf{R}$ be a function, $\tau > 0$.
 1000 Introduce the function $g_1 : [0, \tau] \rightarrow \mathbf{R}$,

$$1001 \quad (166) \quad g_1(t) := \sup_{x \in \mathfrak{V}_1} \mathcal{G}(t, x),$$

1002 and let $\ell : [0, \tau] \rightarrow \mathbf{R}$ be any function such that $\ell(t) > 0$ for $t \in (0, \tau]$ and $\ell(0) = 0$.
 1003 We give sufficient conditions that guarantee that the limit

$$1004 \quad (167) \quad \frac{d}{d\ell} g_1(0^+) := \lim_{t \searrow 0} \frac{g_1(t) - g_1(0)}{\ell(t)}$$

1005 exists. For this purpose we introduce for each t the set of maximisers

$$1006 \quad (168) \quad \mathfrak{V}_1(t) = \{x^t \in \mathfrak{V}_1 : \sup_{x \in \mathfrak{V}_1} \mathcal{G}(t, x) = \mathcal{G}(t, x^t)\}.$$

1007 The next lemma can be found with slight modifications in [7, Theorem 2.1, p. 524].

1008 **LEMMA 6.1.** *Let the following hypotheses be satisfied.*

- 1009 (A1) (i) For all t in $[0, \tau]$ the set $\mathfrak{V}_1(t)$ is nonempty,
 1010 (ii) the limit

$$1011 \quad (169) \quad \partial_\ell \mathcal{G}(0^+, x) := \lim_{t \searrow 0} \frac{\mathcal{G}(t, x) - \mathcal{G}(0, x)}{\ell(t)}$$

1012 exists for all $x \in \mathfrak{V}_1(0)$.

- 1013 (A2) For all real null-sequences (t_n) in $(0, \tau]$ and all sequence (x_{t_n}) in $\mathfrak{V}_1(t_n)$, there
 1014 exists a subsequence (t_{n_k}) of (t_n) , $(x_{t_{n_k}})$ in $\mathfrak{V}_1(t_{n_k})$ and x_0 in $\mathfrak{V}_1(0)$, such
 1015 that

$$1016 \quad (170) \quad \lim_{k \rightarrow \infty} \frac{\mathcal{G}(t_{n_k}, x_{t_{n_k}}) - \mathcal{G}(0, x_{t_{n_k}})}{\ell(t_{n_k})} = \partial_\ell \mathcal{G}(0^+, x_0).$$

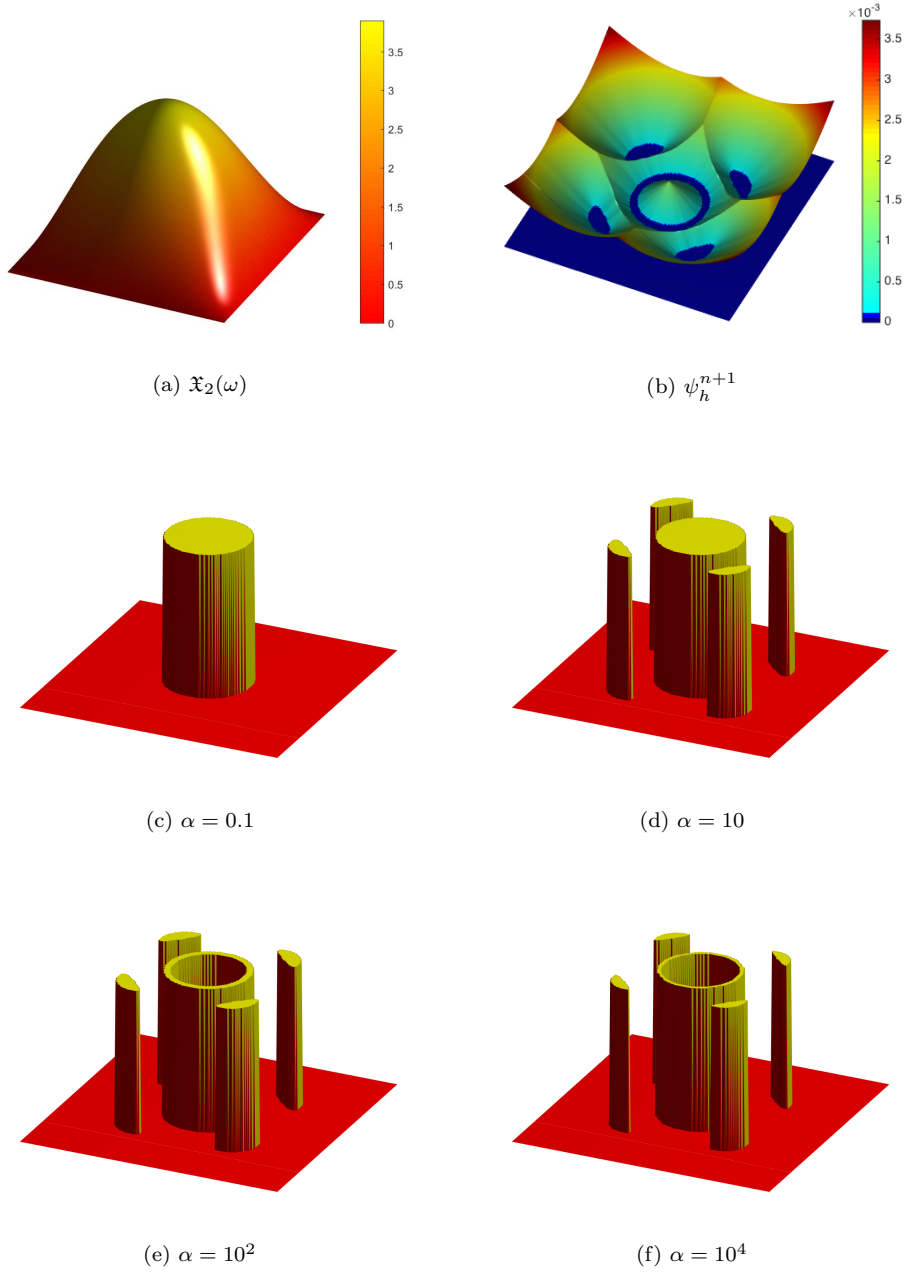


FIG. 10. Test 8. (a) first eigenmode of the Riccati operator. (b) within the level-set method, the actuator is updated according to the zero level-set of the function ψ_h^{n+1} . (c) to (f) optimal actuators for different volume penalties.

1017 Then g_1 is differentiable at $t = 0^+$ with derivative

1018 (171)
$$\frac{d}{dt}g_1(t)|_{t=0^+} = \max_{x \in \mathfrak{B}_1(0)} \partial_t \mathcal{G}(0^+, x).$$

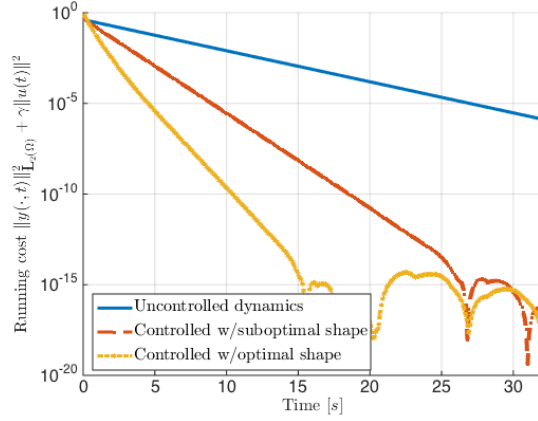


FIG. 11. Test 8. Closed-loop performance for different shapes. The running cost in \mathcal{J}_2 is evaluated for uncontrolled dynamics ($u \equiv 0$), a suboptimal cylindrical actuator of size c located in the center of the domain, and the optimal shape with five components (Figure 10f). Closed-loop dynamics of the optimal shape decay faster.

1019 **Proof of Lemma 3.17.** Our strategy is to prove Lemma 3.17 by applying
 1020 Lemma 6.1 to the function $\mathcal{G}(t, y) := \inf_{x \in \mathfrak{X}} G(t, x, y)$ with $\mathfrak{X}_1 := \mathfrak{X}$. This will
 1021 show that $g(t) := \sup_{y \in \mathfrak{Y}} \mathcal{G}(t, y)$ is right-differentiable at $t = 0^+$. By construction
 1022 Assumption (A0) of Lemma 3.17 is satisfied.

1023 Step 1: For every $t \in [0, \tau]$ and $y \in \mathfrak{Y}$ we have $\mathcal{G}(t, y) = G(t, x^{t,y}, y)$. Hence

$$\begin{aligned}
 \mathcal{G}(t, y) - \mathcal{G}(0, y) &= G(t, x^{t,y}, y) - G(0, x^{0,y}, y) \\
 &= G(t, x^{t,y}, y) - G(0, x^{t,y}, y) + \underbrace{G(0, x^{t,y}, y) - G(0, x^{0,y}, y)}_{\geq 0} \\
 &\geq G(t, x^{t,y}, y) - G(0, x^{t,y}, y)
 \end{aligned}$$

1024 (172)

1025 and similarly

$$\begin{aligned}
 \mathcal{G}(t, y) - \mathcal{G}(0, y) &= G(t, x^{t,y}, y) - G(0, x^{0,y}, y) \\
 &= \underbrace{G(t, x^{t,y}, y) - G(t, x^{0,y}, y)}_{\leq 0} + G(t, x^{0,y}, y) - G(0, x^{0,y}, y) \\
 &\leq G(t, x^{0,y}, y) - G(0, x^{0,y}, y).
 \end{aligned}$$

1026 (173)

1027 Therefore using Assumption (A2) of Lemma 3.17 we obtain from (99) and (100)

$$\liminf_{t \searrow 0} \frac{\mathcal{G}(t, y) - \mathcal{G}(0, y)}{\ell(t)} \geq \partial_t G(0^+, x^{0,y}, y) \geq \limsup_{t \searrow 0} \frac{\mathcal{G}(t, y) - \mathcal{G}(0, y)}{\ell(t)}.$$

1028 (174)

1029 Hence Assumption (A1) of Lemma 6.1 is satisfied.

1030 Step 2: For every $t \in [0, \tau]$ and $y^t \in \mathfrak{Y}(t)$ we have $\mathcal{G}(t, y^t) = G(t, x^{t,y^t}, y^t)$ and

1031 hence

(175)

$$\begin{aligned}
 \mathcal{G}(t, y^t) - \mathcal{G}(0, y^t) &= G(t, x^{t, y^t}, y^t) - G(0, x^{0, y^t}, y^t) \\
 &= G(t, x^{t, y^t}, y^t) - G(0, x^{t, y^t}, y^t) + \underbrace{G(0, x^{t, y^t}, y^t) - G(0, x^{0, y^t}, y^t)}_{\geq 0} \\
 &\geq G(t, x^{t, y^t}, y^t) - G(0, x^{t, y^t}, y^t)
 \end{aligned}$$

1033 and similarly

(176)

$$\begin{aligned}
 \mathcal{G}(t, y^t) - \mathcal{G}(0, y^t) &= \underbrace{G(t, x^{t, y^t}, y^t) - G(t, x^{0, y^t}, y^t)}_{\leq 0} + G(t, x^{0, y^t}, y^t) - G(0, x^{0, y^t}, y^t) \\
 &\leq G(t, x^{0, y^t}, y^t) - G(0, x^{0, y^t}, y^t).
 \end{aligned}$$

1035 Thanks to Assumption (A3) of Lemma 3.17 For all real null-sequences (t_n) in $(0, \tau]$
 1036 and all sequences $(y^{t_n}), y^{t_n} \in \mathfrak{Y}(t_n)$, there exists a subsequence (t_{n_k}) of (t_n) , $(y^{t_{n_k}})$
 1037 of (y^{t_n}) , and y^0 in $\mathfrak{Y}(0)$, such that

$$(177) \quad \lim_{k \rightarrow \infty} \frac{G(t_{n_k}, x^{t_{n_k}, y^{t_{n_k}}}, y^{t_{n_k}}) - G(0, x^{t_{n_k}, y^{t_{n_k}}}, y^{t_{n_k}})}{\ell(t_{n_k})} = \partial_\ell G(0^+, x^{0, y^0}, y^0)$$

1039 and

$$(178) \quad \lim_{k \rightarrow \infty} \frac{G(t_{n_k}, x^{0, y^{t_{n_k}}}, y^{t_{n_k}}) - G(0, x^{0, y^{t_{n_k}}}, y^{t_{n_k}})}{\ell(t_{n_k})} = \partial_\ell G(0^+, x^{0, y^0}, y^0).$$

1041 Hence choosing $t = t_{n_k}$ in (175) we obtain

$$\begin{aligned}
 &\liminf_{k \rightarrow \infty} \frac{\mathcal{G}(t_{n_k}, y^{t_{n_k}}) - \mathcal{G}(0, y^{t_{n_k}})}{\ell(t_{n_k})} \\
 (179) \quad &\stackrel{(175)}{\geq} \liminf_{k \rightarrow \infty} \frac{G(t_{n_k}, x^{t_{n_k}, y^{t_{n_k}}}, y^{t_{n_k}}) - G(0, x^{t_{n_k}, y^{t_{n_k}}}, y^{t_{n_k}})}{\ell(t_{n_k})} \\
 &\stackrel{(177)}{=} \partial_\ell G(0^+, x^{0, y^0}, y^0)
 \end{aligned}$$

1043 and similarly choosing $t = t_{n_k}$ in (176) we get

$$\begin{aligned}
 &\limsup_{k \rightarrow \infty} \frac{\mathcal{G}(t_{n_k}, y^{t_{n_k}}) - \mathcal{G}(0, y^{t_{n_k}})}{\ell(t_{n_k})} \\
 (180) \quad &\stackrel{(176)}{\leq} \limsup_{k \rightarrow \infty} \frac{G(t_{n_k}, x^{0, y^{t_{n_k}}}, y^{t_{n_k}}) - G(0, x^{0, y^{t_{n_k}}}, y^{t_{n_k}})}{\ell(t_{n_k})} \\
 &\stackrel{(178)}{=} \partial_\ell G(0^+, x^{0, y^0}, y^0).
 \end{aligned}$$

1045 Combining (179) and (180) we conclude that

$$(181) \quad \lim_{k \rightarrow \infty} \frac{\mathcal{G}(t_{n_k}, y^{t_{n_k}}) - \mathcal{G}(0, y^{t_{n_k}})}{\ell(t_{n_k})} = \partial_\ell G(0^+, x^{0, y^0}, y^0),$$

1047 which is precisely Assumption (A2) of Lemma 6.1.

1048 Step 1 and Step 2 together show that Assumptions (A1) and (A2) of Lemma 6.1
 1049 are satisfied and this finishes the proof.

1050

REFERENCES

- 1051 [1] A. ALLA, M. FALCONE, AND D. KALISE, *An efficient policy iteration algorithm for the solution*
 1052 *of dynamic programming equations*, SIAM J. Sci. Comput., 35 (2015), pp. A181–A200.
- 1053 [2] G. ALLAIRE, F. JOUVE, AND A.-M. TOADER, *Structural optimization using sensitivity analysis*
 1054 *and a level-set method*, J. Comput. Phys., 194 (2004), pp. 363–393.
- 1055 [3] S. AMSTUTZ, *Augmented Lagrangian for cone constrained topology optimization*, Comput.
 1056 *Optim. Appl.*, 49 (2011), pp. 101–122, <https://doi.org/10.1007/s10589-009-9272-3>, <http://dx.doi.org/10.1007/s10589-009-9272-3>.
- 1057 [4] S. AMSTUTZ AND H. ANDRÄ, *A new algorithm for topology optimization using a level-set*
 1058 *method*, J. Comput. Phys., 216 (2006), pp. 573–588, <https://doi.org/10.1016/j.jcp.2005.12.015>,
 1059 <http://dx.doi.org/10.1016/j.jcp.2005.12.015>.
- 1060 [5] A. BENSOUSSAN, *Optimization of sensors' location in a distributed filtering problem*,
 1061 Springer Berlin Heidelberg, Berlin, Heidelberg, 1972, pp. 62–84, <https://doi.org/10.1007/BFb0064935>.
- 1062 [6] M. C. DELFOUR AND J.-P. ZOLÉSIO, *Shape sensitivity analysis via min max differentiability*,
 1063 SIAM J. Control Optim., 26 (1988), pp. 834–862, <https://doi.org/10.1137/0326048>, <http://dx.doi.org/10.1137/0326048>.
- 1064 [7] M. C. DELFOUR AND J.-P. ZOLÉSIO, *Shapes and geometries: Metrics, analysis, differential cal-*
 1065 *culus, and optimization*, Society for Industrial and Applied Mathematics (SIAM), Philadel-
- 1066 phia, PA, second ed., 2011.
- 1067 [8] V. F. DEM'YANOV AND V. N. MALOZĚMOV, *Einführung in Minimax-Problem*, Akademische
 1068 Verlagsgesellschaft Geest & Portig K.-G., 1975. German translation.
- 1069 [9] A. EL JAÏ AND A. J. PRITCHARD, *Sensors and controls in the analysis of distributed systems*,
 1070 Ellis Horwood Series: Mathematics and its Applications, Ellis Horwood Ltd., Chichester;
 1071 Halsted Press [John Wiley & Sons, Inc.], New York, 1988. Translated from the French by
 1072 Catrin Pritchard and Rhian Pritchard.
- 1073 [10] L. C. EVANS, *Partial differential equations*, vol. 19 of Graduate Studies in Mathematics, Amer-
 1074 ican Mathematical Society, Providence, RI, 1998.
- 1075 [11] F. FAHROO AND M. A. DEMETRIOU, *Optimal actuator/sensor location for active noise*
 1076 *regulator and tracking control problems*, J. Comput. Appl. Math., 114 (2000),
 1077 pp. 137–158, [https://doi.org/10.1016/S0377-0427\(99\)00293-9](https://doi.org/10.1016/S0377-0427(99)00293-9), [http://dx.doi.org/10.1016/S0377-0427\(99\)00293-9](http://dx.doi.org/10.1016/S0377-0427(99)00293-9). Control of partial differential equations (Jacksonville, FL, 1998).
- 1078 [12] M. I. FRECKER, *Recent advances in optimization of smart structures and actuators*, Journal
 1079 of Intelligent Material Systems and Structures, 14 (2003), pp. 207–216, <https://doi.org/10.1177/1045389X03031062>, <http://dx.doi.org/10.1177/1045389X03031062>, <https://arxiv.org/abs/http://dx.doi.org/10.1177/1045389X03031062>.
- 1080 [13] P. HÉBRARD AND A. HENROT, *A spillover phenomenon in the optimal location of ac-*
 1081 *tuator*, SIAM J. Control Optim., 44 (2005), pp. 349–366, <https://doi.org/10.1137/S0363012903436247>, <http://dx.doi.org/10.1137/S0363012903436247>.
- 1082 [14] M. HINTERMÜLLER, C. N. RAUTENBERG, M. MOHAMMADI, AND M. KANITSAR, *Optimal sensor*
 1083 *placement: a robust approach*, WIAS preprint, (2016), p. 34 pp., http://www.wias-berlin.de/preprint/2287/wias_preprints_2287.pdf.
- 1084 [15] K. ITO, K. KUNISCH, AND G. H. PEICHL, *Variational approach to shape derivatives*, ESAIM
 1085 Control Optim. Calc. Var., 14 (2008), pp. 517–539, <https://doi.org/10.1051/cocv:2008002>,
 1086 <http://dx.doi.org/10.1051/cocv:2008002>.
- 1087 [16] D. KASINATHAN AND K. MORRIS, \mathbb{H}_∞ -optimal actuator location, IEEE Trans. Automat. Con-
 1088 trol, 58 (2013), pp. 2522–2535, <https://doi.org/10.1109/TAC.2013.2266870>, <http://dx.doi.org/10.1109/TAC.2013.2266870>.
- 1089 [17] LAURAIN, A. AND STURM, K., *Distributed shape derivative via averaged adjoint method and*
 1090 *applications*, ESAIM: M2AN, 50 (2016), pp. 1241–1267.
- 1091 [18] K. MORRIS, *Linear-quadratic optimal actuator location*, IEEE Trans. Automat. Control, 56
 1092 (2011), pp. 113–124, <https://doi.org/10.1109/TAC.2010.2052151>, <http://dx.doi.org/10.1109/TAC.2010.2052151>.
- 1093 [19] K. MORRIS, M. A. DEMETRIOU, AND S. D. YANG, *Using \mathbb{H}_2 -control performance metrics for*
 1094 *the optimal actuator location of distributed parameter systems*, IEEE Trans. Automat.
 1095 Control, 60 (2015), pp. 450–462, <https://doi.org/10.1109/TAC.2014.2346676>, <http://dx.doi.org/10.1109/TAC.2014.2346676>.
- 1096 [20] A. A. NOVOTNY AND J. SOKOŁOWSKI, *Topological derivatives in shape optimization*, Interac-
 1097 tion of Mechanics and Mathematics, Springer, Heidelberg, 2013, <https://doi.org/10.1007/978-3-642-35245-4>, <http://dx.doi.org/10.1007/978-3-642-35245-4>.
- 1098 [21] Y. PRIVAT, E. TRÉLAT, AND E. ZUAZUA, *Actuator design for parabolic distributed parameter*
 1099

- 1111 *systems with the moment method*, SIAM J. Control Optim., 55 (2017), pp. 1128–1152,
1112 <https://doi.org/10.1137/16M1058418>, <http://dx.doi.org/10.1137/16M1058418>.
- 1113 [22] J. SOKOŁOWSKI AND A. ŻOCHOWSKI, *On the topological derivative in shape optimization*, SIAM
1114 J. Control Optim., 37 (1999), pp. 1251–1272, <https://doi.org/10.1137/S0363012997323230>,
1115 <http://dx.doi.org/10.1137/S0363012997323230>.
- 1116 [23] K. STURM, *Minimax Lagrangian approach to the differentiability of nonlinear PDE constrained*
1117 *shape functions without saddle point assumption*, SIAM J. Control Optim., 53 (2015),
1118 pp. 2017–2039, <https://doi.org/10.1137/130930807>, <http://dx.doi.org/10.1137/130930807>.
- 1119 [24] K. STURM, *Shape differentiability under non-linear PDE constraints*, in *New trends in shape*
1120 *optimization*, vol. 166 of *Internat. Ser. Numer. Math.*, Birkhäuser/Springer, Cham, 2015,
1121 pp. 271–300, https://doi.org/10.1007/978-3-319-17563-8_12, <http://dx.doi.org/10.1007/>
1122 [978-3-319-17563-8_12](http://dx.doi.org/10.1007/978-3-319-17563-8_12).
- 1123 [25] F. TRÖLTZSCH, *Optimale Steuerung partieller Differentialgleichungen: Theorie, Verfahren und*
1124 *Anwendungen*, Vieweg, 2005, https://books.google.de/books?id=7_pXfkEbkdEC.
- 1125 [26] S. VALADKHAN, K. MORRIS, AND A. KHAJEPOUR, *Stability and robust position control of hys-*
1126 *teretic systems*, *Internat. J. Robust Nonlinear Control*, 20 (2010), pp. 460–471, <https://doi.org/10.1002/rnc.1457>, <http://dx.doi.org/10.1002/rnc.1457>.
- 1127 [27] M. VAN DE WAL AND B. DE JAGER, *A review of methods for input/output selection*, *Automatica*
1128 *J. IFAC*, 37 (2001), pp. 487–510, [https://doi.org/10.1016/S0005-1098\(00\)00181-3](https://doi.org/10.1016/S0005-1098(00)00181-3), [http://dx.doi.org/10.1016/S0005-1098\(00\)00181-3](http://dx.doi.org/10.1016/S0005-1098(00)00181-3).
- 1129 [28] J. WLOKA, *Partielle Differentialgleichungen*, B. G. Teubner, Stuttgart, 1982. Sobolevräume
1130 und Randwertaufgaben. [Sobolev spaces and boundary value problems], *Mathematische*
1131 *Leitfäden*. [Mathematical Textbooks].
1132
1133